ROTORCRAFT NOISE - STATUS AND RECENT DEVELOPMENTS

Albert R. George
Professor
Ben Wel-C. Sim, and David R. Polak
Graduate Research Assistants

Cornell University
Mechanical & Aerospace Engineering Department
Ithaca, New York 14853-7501
U.S.A.

Submitted to Pacific International Conference on Aerospace Science and Technology (PICAST'1 1993), December 6-9, 1993, National Cheng Kung University, Tainan, Taiwan, Republic of China. Paper number 930292.

ROTORCRAFT NOISE - STATUS AND RECENT DEVELOPMENTS

Albert R. George
Professor
Ben W.-C. Sim, and David R. Polak
Graduate Research Assistants

Cornell University
Ithaca, NY 14853-7501
U.S.A.

ABSTRACT

Because of the wide variety of rotor noise generation mechanisms, such as transonic flow, wake interaction, flow separation, turbulence-surface interactions, recirculation, etc., a wide range of noise prediction methodologies need to be developed in order to satisfactorily predict rotorcraft noise. Satisfactory predictions are a prerequisite to developing noise reduction strategies. However, the state-of-the-art has not yet reached the stage where predictions can be made with acceptable confidence for all mechanisms.

This paper briefly reviews rotorcraft noise mechanisms and their approximate importance for different types of rotorcraft in different flight regimes. Discrete noise is due to periodic flow disturbances and includes impulsive noise produced by phenomena which occur during a limited segment of a blade's rotation. Broadband noise results when rotors interact with random disturbances, such as turbulence, which can originate in a variety of sources. The status of analysis techniques for these mechanisms will be reviewed. Also, some recent progress will be presented on the understanding and analysis of tilt rotor aircraft noise due to: (1) Recirculation and blockage effects of the rotor flow in hover (2) Blade-vortex interactions in forward and descending flight.

NOMENCLATURE

ρ = density
c_o = undisturbed sound speed
Q = mass source strength (mass/volume.time)
F_i = force/volume (momentum/volume.time)
T_{ij} = Lighthill stress tensor, $\rho u_i u_j + (p - c_o^2 \rho)\,\delta_{ij} - \sigma_{ij}$
σ_{ij} = viscous stress tensor
p_{ij} = $p\delta_{ij} - \sigma_{ij}$
R = $| x_i - x_i' | = c_o(t - t')$
M_{tip} = tip Mach number
M_t = BVI trace Mach number

1.0 INTRODUCTION

The noise generated by helicopters and other rotorcraft is a critical factor in the acceptability and economics of these vehicles. Tilt rotor aircraft and helicopters both have high potential for use as medium-range transports in areas where airport terminal land is difficult to develop due to high population density. In order to be successful in such areas rotorcraft must be designed to be operable with acceptable noise impact on nearby residents. Lowson (1992) describes current International Civil Air Organization (ICAO) helicopter certification requirements, and the present conservative approach adopted by manufacturers to meet them. As will become evident, this conservative (and hence non-optimal) approach stems from an inability to accurately predict rotorcraft noise in all flight regimes.

There are a variety of noise sources associated with rotorcraft, and their relative importance depends upon the particular vehicle design and its operating conditions, as summarized by Martin (1989). Indeed, a considerable reduction in radiated noise is possible by careful choice of operating conditions (George et al., 1989, Lowson, 1992). Rotorcraft engines produce noise of various types which are not treated in this paper. This paper concerns the present state of understanding and prediction abilities for rotor noise generated by aerodynamics. Some earlier reviews of helicopter and rotor noise are given by Hubbard et al. (1971), George (1978), White (1980), Leverton (1989), Schmitz (1991) and Lowson (1992). Sources of rotor noise include steady, periodic and random loads on the rotor blades, as well as volume displacement and nonlinear aerodynamic effects at high blade Mach numbers. Either main or tail rotors can be dominant noise sources at various frequencies and observer positions. Figure 1 presents a simplified overview of rotor noise generation mechanisms.

Subjective response to conventional rotorcraft noise is generally expressed in terms of perceived noise levels (PNdB) or a weighted sound level (dBA, dBD) with modifications to account for sound duration and tonal components (EPNdB). These weighted sound metrics account for the fact that higher frequencies are generally more annoying, as is intermittent or irregular noise or pure tones. In addition, the external noise generated by an aircraft usually propagates for some distance through the atmosphere before reaching observers, thus undergoes frequency-dependent absorption, which effectively damps out some high frequency noise components. Thus, for the flyover case, the important range for annoyance tends to fall in the low to middle frequency range (100 - 2000 Hz). Of course for a rotorcraft in takeoff, approach, or near-ground hover flight, the source-observer propagation distances can be much less, so that higher frequency noise can contribute significantly to annoyance in these cases.

Figure 2 shows a typical helicopter noise spectrum and waveform and indicates some of the acoustic sources listed above and shown diagrammatically in Figure 1. Low frequency noise is dominated by the main rotor with peaks at the blade passing frequency, its first few harmonics, and at frequencies between, due to steady loads and ingested turbulence and disturbances. Tail rotor and turbulence induced broadband noise occupy the mid-frequency ranges. Lowson (1992) lists the approximate order of importance of helicopter rotor noise sources as

1) high speed impulsive noise (when it occurs)
2) blade vortex interaction noise during maneuver or low speed descent
3) turbulence induced noise
4) tail rotor noise
5) other main rotor discrete frequency noise

Lowson's ranking can be regarded as an appropriate acoustic guideline for the design of new helicopters, and relates to the present research emphasis in rotor acoustics.

In addition to the helicopter noise sources described above, tilt rotor aircraft have several novel features which affect their aeroacoustic characteristics (George et al., 1989). In various flight modes the rotor and rotor-wake aerodynamics of these vehicles are different from either helicopters or conventional aircraft. During the operation of a tilt rotor aircraft, additional degree of freedom, such as nacelle tilt, affect the rotor aerodynamics and thus noise (George et al., 1989). Along with operational degrees of freedom, tilt rotor aircraft have several other interesting acoustic effects compared to helicopters: (1)

different paths of the tip vortices in the wake (2) higher disk loading (3) phasing between signals from the two rotors (George et al., 1989) (4) variable orientations of the rotors and nacelles with respect to observers (5) effects of the wing-rotor wake flow on the rotor (6) blade loading differences due to high blade twist, and (7) close passage of blade tips to the fuselage in airplane mode.

With such a wide variety of acoustic sources, operating conditions and vehicle configurations, it is not surprising that rotor noise predictions cannot yet be made with satisfactory confidence. Nevertheless, significant progress has been made. The next section briefly reviews aeroacoustic theory and computational methods. Next, a review of rotor noise mechanisms will be given, emphasizing recent progress. This is followed by a section on some recent progress on the understanding and prediction of tilt rotor noise. Finally, a brief discussion on noise reduction techniques will be presented.

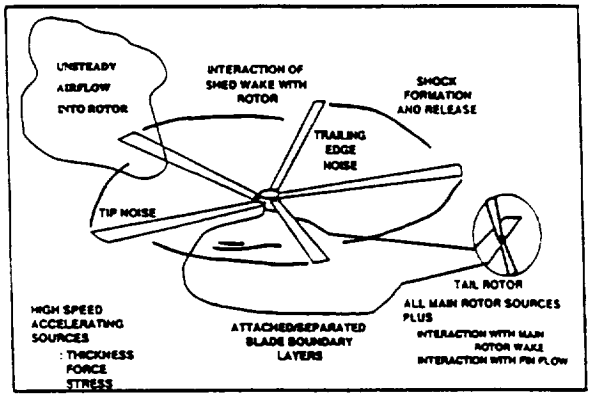

Figure 1. Basic mechanisms of rotor noise generation (from Lowson, 1992).

2.0 AEROACOUSTIC NOISE THEORY

To understand the mechanisms which lead to acoustic radiation from rotors, consider Lighthill's acoustic analogy. This formulation manipulates the exact equations of fluid mechanics into a conceptually simple form. Beginning from the equations of mass and momentum conservation, but allowing for mass sources and applied forces in the fluid, Lighthill (1952) showed that these equations could be put in the form of a wave equation on the left side with all other terms on the right side:

$$\frac{\partial^2 \rho}{\partial t^2} - c_o^2 \frac{\partial^2 \rho}{\partial x_i^2} = \frac{\partial Q}{\partial t} - \frac{\partial F_i}{\partial x_i} + \frac{\partial^2 T_{ij}}{\partial x_i \partial x_j} \qquad (1)$$

Lighthill's contribution was the simplifying concept of considering the right hand side of this equation as known source terms. In fact, these terms are rarely known exactly, but can often be satisfactorily estimated. The acoustic analogy provides a major simplification by separating the problems of aerodynamics and acoustics. If the right hand side is written as a known function $g(x_i,t)$ then the inhomogeneous wave equation (1) can be simply solved for the radiated sound. The actual effects of fluid motion and solid boundaries in the generation and propagation of sound are modeled by sources in an undisturbed fluid. In this formulation we consider the moving rotor blades and their associated flow fields as being comprised of (i) moving sources and sinks (Q) to model the motion of the rotor blade volumes, (ii) moving forces (F_i) to model the motion of the forces between the blades and the fluid, and (iii) a moving T_{ij} distribution which accounts for nonlinear flow effects. T_{ij} can include such effects as turbulence, compressible flow and shock wave effects, non-isentropic effects and viscous flow effects. When using Lighthill's analogy in the form of equation (1) the various source and force terms are generally assumed to act as point sources or to be distributed over the blade mean rotational plane, or the mean helical surface swept out by the rotor or propeller motion. If a more complete representation of moving bodies is desired, it is generally better to work with the Ffowcs Williams and Hawkings (1969) form of the Lighthill equation. Either equation (1) or the Ffowcs Williams and Hawkings equation can be written as an inhomogeneous wave equation of the form

$$\frac{\partial^2 \rho}{\partial t^2} - c_o^2 \frac{\partial^2 \rho}{\partial x_i^2} = g(x_i,t) \qquad (2)$$

whose formal solution can be written as

$$\rho - \rho_o = \frac{1}{4\pi c_o^2} \iiint d^3x_i' \int dt' \; g(x_i',t') \frac{\delta\left(t - \frac{R}{c_o} - t'\right)}{R} \qquad (3)$$

Using the properties of the delta function this may be written either in terms of retarded times

$$\rho - \rho_o = \frac{1}{4\pi c_o^2} \iiint d^3x_i \frac{g\left(x_i', t - \frac{R}{c_o}\right)}{R} \qquad (4)$$

or it can be expressed in terms of an integral over past times of contributions on a contracting spherical surface Ω of radius R, implying that g is evaluated on this surface $x_i'(t')$. Then

$$\rho - \rho_o = \frac{1}{4\pi c_o^2} \int dt' \iint d^2\Omega \frac{g(x_i'(t'),t')}{R} \qquad (5)$$

From this form, it is easy to see how the different terms in the right hand side of (1) contribute to the far-field sound.

Stationary sources clearly contribute only if unsteady. Also, the force term (F_i in equation (1)) is differentiated in the x_i direction. Thus the variation of the force components in their own respective directions contribute to sound. Finally, the last of the three terms on the right side of the Lighthill equation is the derivative of T_{ij}, where $T_{ij} = \rho u_i u_j + (p - c_o^2 \rho)\,\delta_{ij} - \sigma_{ij}$. The terms in T_{ij} are, respectively, nonlinear flow contributions, non-isentropic effects and viscous stress effects. Again, the contributions are important only if the T_{ij} components in the observer's direction vary significantly due to either blade rotation or unsteadiness during the passage of time of the Ω surface through the disturbed flow region. In all cases, as the body moves with a relative velocity closer to the speed of sound towards the observer, the Ω surface will spend more and more time passing through the body, allowing more time for each term on the right side of the Lighthill equation to vary due to the ensuing blade motion, and hence contribute to acoustic radiation.

Several rotorcraft noise prediction programs have been developed based on the Ffowcs-Williams and Hawking's equation. This includes NASA's WOPWOP code (Brentner, 1986) and the U.S. Army's RAPP (Gallman, 1990). These programs model rotor blade thickness noise with non-compact monopoles and local blade surface pressure with distributed dipoles. Dunn and Farassat (1990) have shown that by re-formulating the Ffowcs-Williams and Hawkings equation (Farassat's formulation 3), thickness noise for transonic propellers can be calculated more accurately and efficiently. This modified analysis can be extended to other sources of rotor /propeller noise as well. Recently, the effect of quadrupole shock noise has been added to WOPWOP (Farassat et al., 1991, Tadghighi et al., 1991) to improve noise prediction at high tip speeds. NASA Langley has also developed a full system rotorcraft noise/performance prediction code (ROTONET) to allow the incorporation of the best available noise control and evaluation technology into new helicopter designs (Weir and

Golub, 1989). An overall review of current rotor noise prediction status is documented in Brentner and Farassat (1992).

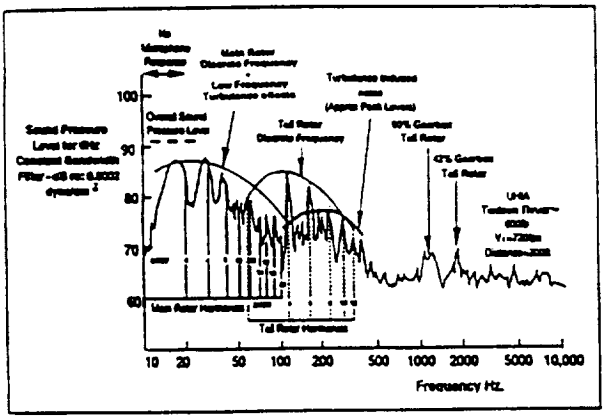

Figure 2. Typical helicopter noise spectrum (from Schmitz, 1991).

3.0 ROTOR NOISE MECHANISMS

This section reviews rotor noise mechanisms, emphasizing recent progress. For convenience, the mechanisms have been separated into three categories: (1) blade volume (thickness) (2) blade loading (3) quadrupole noise. This classification corresponds to the three source terms in Lighthill's inhomogeneous wave equation, equation (1). A fairly inclusive table of the noise sources and their mechanisms are shown below.

Noise	Mechanism	Modeling
Discrete	Blade Volume	Thickness
	Blade Steady Forces	Loading
	Blade Periodic Forces	Loading
BVI Impulsive	Subsonic BVI	Loading
	Transonic BVI with Shocks	Loading and Quadrupole
Broadband	Self-Generated Turbulence (Trailing Edge Noise)	Loading
	Vortex Shedding	Loading
	Inflow Turbulence	Loading
	Mean Flow Turbulence	Quadrupole
High-Speed Impulsive (HSI)	"Compressibility" Shocks	Quadrupole

3.1 Noise due to Blade Volume

Blade thickness (or volume) causes far-field noise because of the difference in retarded time of pressure fluctuations due to the motion of the blade volume. The first analysis of thickness effects on rotating radiated sound was made by Deming (1938). His analysis is essentially complete for a simple stationary propeller with symmetric blades, but includes some rough approximations regarding blade profile shapes. Classical acoustical treatment of moving bodies generally dismissed the importance of thickness noise. However this was found not to be the case for high speed rotors where volume displacement effects begin to dominate. More sophisticated analyses for the high speed case were reported by Hawkings and Lowson (1974), and Farassat (1975) using non-compact monopole terms to represent thickness and distributed dipoles to represent localized pressures. These analyses alone agree fairly well with non-lifting blade experiments, although some discrepancies are apparent, particularly for high advancing blade Mach numbers.

3.2 Noise due to Blade Forces

In this section, the present state of knowledge regarding noise generated by blade loading will be reviewed. Steady, periodic and random blade forces can all contribute to rotor noise. The resulting noise can either be impulsive or broadband.

3.2.1 Steady Forces

The radiation due to steady thrust (lift) and torque (drag) forces was first analyzed by Gutin (1936). He modeled the forces as constant but moving point dipole acoustic sources, and the resulting discrete spectrum decays very rapidly with frequency. Gutin's theory alone predicts the first few harmonics of the rotor noise correctly but severely underestimates the measured higher frequency harmonics, especially for low tip speeds. Clearly, this theory is not adequate for helicopters where the main rotor fundamental frequency is on the order of 15 Hertz, implying that only the higher harmonics are important for annoyance and audibility.

3.2.2 Periodic Blade Loadings - Rotational Noise

The problem with the Gutin theory was resolved considerably later when Lowson and Ollerhead (1969) and Wright (1969) analyzed the radiation due to azimuthal variations in blade loading which are steady in time. They found that the higher harmonics of the blade loading spectrum are extremely important to high frequency discrete spectrum rotational noise. In fact at high frequencies the sound from even very small amplitude loading harmonics dominates that due to the steady loading analyzed by Gutin. Although these analyses related the high harmonics in the noise spectra to high frequency blade loading harmonics, they did not explain the origin of all the measured or inferred high frequency loading harmonics. For lower order loading harmonics one can invoke forward flight, fuselage effects, cyclic blade motions, and cyclic blade incidence changes, but it is generally necessary to use experimental or empirical high frequency loading laws to get agreement with experiment. In addition, measured spectra show a peak-valley rather than a line structure implying random rather than periodic loadings.

For some helicopters, tail rotor rotational noise can be more important than main rotor noise in certain parts of the spectrum. This is typically from 100 to 500 hertz, a range which is very important to audibility and annoyance. Tail rotors tend to produce a large number of rotational harmonics as their inflow is generally quite non-uniform due to ingestion of the main rotor wake and the influence of the nearby tail boom or pylon on the flow. However, reduction in tip speed is quite useful in reducing this radiation.

3.2.3 Blade-Vortex Interactions (BVI)

It is known that blade-vortex interaction (BVI) noise is one of the most important sources of rotor radiated noise. Intense BVI noise occurs mostly during flight maneuvers and low power descent. BVI noise is the result of rapid load variations caused by a rotor blade (main or tail rotor) passing at close proximity to or through a tip vortex trailing from the same or another blade. These rapid pressure fluctuations can be considered as dipole sources which radiate acoustic energy, the strength of which is dependent upon the unsteady lift fluctuation on the blade when the blade approaches an isolated vortex. Such interactions produce annoying "blade-slapping" noises in the mid frequencies and are highly directional. The strength of BVI noise is governed by the local tip vortex strength, tip vortex core size, local interaction angle of the blade and vortex line, and the separation distance between the vortex and the blade. Theoretical analyses of the basic aeroacoustic interaction between a blade and vortex have been carried out by Widnall (1971) and Filotas (1973), assuming classical attached flow response of the blade to the additional velocity of the inviscid vortex model. The nature of main rotor BVI disturbances has been investigated experimentally by Cox (1977), Tangler (1977) and Martin et al. (1990). Lee (1985) studied the effect of a turbulent viscous core on the unsteady blade loading. Experiments conducted on the BO-105 helicopter model

by Martin et al. (1988) have indicated the importance of retreating side BVIs, in addition to the advancing side BVIs. More recent BVI studies have focused on assessing the helicopter's operating conditions, such as the rotor's advance ratio and tip-path-plane angle (Burley and Martin, 1988, Splettstoesser et al., 1990) on the amplitude and directionality of BVI noise. However, due to the complexity of the trailing tip vortex geometry and of the blade's actual response, we are far from being able to predict this noise a priori for given helicopter operating conditions.

The success of BVI noise prediction is dependent upon the understanding of the helicopter's aerodynamics in the near and far wake. A realistic rotor wake model is comprised of the blades' bound circulation, trailing helical vorticity (due to radially changing blade loadings) and shed vorticity (due to azimuthally changing blade loading); these are constantly interacting with each other and inducing downwash in the rotor's distorted flow field. Experiments have shown that the near-wake rolls up rapidly upon leaving the blade to form a concentrated vortex similar to a lifting wing in forward flight (Ghee and Elliot, 1992). It has been a general consensus that a rigid wake model is inadequate for BVI noise predictions. The current state of technology in rotor wake evaluation uses experimental data and empirical formulations to form prescribed wake models (Egolf and Langrebe, 1983, Beddoes, 1985). These prescribed wake models are generally better at capturing the wake characteristics but tend to be rotor-specific. With the advent of faster and more efficient computers, free wake calculations have been attempted by Sadler (1971), Scully (1975), Johnson (1981) and Bliss (1989), but are highly complex and time consuming to develop.

Computational fluid dynamics calculations have been recently applied to help address BVI noise predictions. Most of the cases studied involve a rotor airfoil encountering a free vortex in two-dimensional unsteady flow (George and Chang, 1984, Rai, 1987, Sirinivasan and McCroskey, 1987). Numerical computations are also performed based on the unsteady three-dimensional full potential equation by Hassan and Charles (1989), with wake geometry supplied by CAMRAD (Johnson, 1981). Results to date have indicated that linearized small-disturbance simulations of the two-dimensional BVI problem do not adequately represent the aerodynamic near-field. Nonlinear effects must be introduced for better BVI noise predictions.

Another source of BVI noise comes from the interaction between the main rotor wake and the tail rotor blades. Studies developed by Leverton (1982) and George et al. (1986) modeled the phenomenon on the assumption of a flat blade chopping through a skewed vortex filament generated by the main rotor. Again, the validity of these predictions rely heavily on the details of the approaching wake as in the case of the main rotor's BVI. In addition, the tail rotor flow field is further complicated by separated flows (Tadghighi, 1989) from the fuselage, fin, engines, etc. Designs to minimize this noise source have focused on positioning the tail rotor in as clean a flow as possible under all flight conditions. A revolutionary concept is to remove the tail rotor completely and replace it with small jet reaction and aerodynamic control, such as the one on the McDonnell Douglas's NOTAR helicopter.

3.2.4 Stall & Shock Effects in BVI

It has also been recognized that during blade vortex interactions other effects can occur in addition to the loading variations due to classical subsonic attached flow. Unsteady stall can be caused by local flow incidence changes, and shock wave formation can be caused by increased flow velocity (Tangler, 1977). It is reasoned that the interacting vortex induced stall on the blade, usually on the retreating side, which in turn generated high frequency vortex shedding. On the other hand, shock waves are usually formed on the advancing side during high speed motion. This phenomena, typically known as transonic BVI, gives drastically different loadings than found from classical analyses and also exhibit considerably more rapid changes in loading. Such rapid time variations in loading generate strong acoustic radiation especially when the advancing tip Mach number of the rotor approaches transonic values. McCroskey and Goorjian (1983) and George and Chang (1984) have analyzed unsteady, transonic, two-dimensional interaction flow fields using a numerical, small-disturbance approach, including the introduction of finite core size vortices which are convected by the local disturbed flow. Sirinivasan et al. (1985) also studied this flow using a numerical thin-layer Navier-Stokes approach. More recent studies by Obermeier (1991) and Lent et al. (1990) have suggested three separate sources of shock radiation. The first is a "compressibility" shock at the leading edge which is formed as the vortex passes beneath the rotor blade. Generation of noise due to "compressibility" shock is directly related to the unsteady thickness noise radiation by the rotor. The second is a shock which can be caused by separation from the blade at sufficiently large induced angle of attack. The third source of shock radiation is the "transonic" shock formed on the underside of the blade due to the presence of local supersonic flow. Research by Tijdeman (1977), George and Chang (1984) and Lyrintzis and George (1989) have showed that for supersonic flow conditions, shocks formed from vortex interaction will be released from the blade surface and propagate into the mid-field. Lyrintzis and George (1989) also showed that the strength of the shocks formed is related to the thickness of the nose of the airfoil. More recently, studies by Lyrintzis and Xue (1991) on unsteady shock motions have illustrated the effects of fluctuating lift and drag coefficients on transonic BVI noise directivity. For all of these factors, as in the basic blade-vortex interaction, the best noise control technique undoubtedly lies in trying to devise a way to eliminate the close passage of the blade and a concentrated vortex rather than in changes which would only affect the details of the aeroacoustic interaction. However, studies indicate that ensuring the local velocity on the blade (including vortex induced velocities) remains subsonic reduces high speed impulsive BVI noise substantially (Lowson, 1976).

3.2.5 Radiation Due to Vortex Streets & Related Phenomena

Any fluctuating forces on a body give rise to sound radiation. One of the first such mechanisms identified was the von Kármán vortex street phenomenon which occurs downstream of circular cylinders and other bluff bodies in certain Reynolds number ranges. Although rotor blades are generally streamlined in shape, load fluctuations associated with nearly periodic vortex shedding can occur. The nearly periodic nature of the fluctuations gives rise to high frequency broadband noise, which is most severe in the case of blunt trailing edges, as shown by Brooks and Schlinker (1983), for example. However, this source occurs only when the boundary layer on at least one side of the airfoil is laminar (Paterson et al., 1973).

3.2.6 Self-Generated Turbulent Loading

Random blade loadings can be generated by the interaction between a rotor blade and the turbulence generated by that blade's own motion, and occur primarily at the blade's trailing edge. The acoustic radiation caused by these interactions is called self-noise. The most obvious example is the turbulent boundary layer on the blade surface. Turbulence passing over an infinite flat surface is a relatively weak sound source, but when turbulent eddies pass over the trailing edge of the blade, somewhat more sound is radiated. Various analyses, by Ffowcs-Williams and Hall (1970), Chase (1972), Jones (1972), Tam and Yu (1975), Amiet (1976) and Kim and George (1982), differ on items such as whether to apply the Kutta condition and its importance, and on the locations, convection speeds and types of multipole sources. According to these analyses, turbulent boundary layer noise is often important compared to incident turbulence noise, which will be discussed in the next section. Kim and George (1982) and Brooks et al. (1989) also demonstrate that self noise can dominate the rotor acoustic spectra in the mid and high

frequencies, in the absence of other sources. The relative importance of inflow versus boundary layer turbulence is related to different intensities and length scales characterizing the phenomena.

Other self-noise sources include turbulence in locally stalled regions (Paterson et al., 1975), tip flow effects (Lowson, 1973, Hoffman et al., 1971), and vortex shedding, as described above. Brooks and Schlinker (1983) review these acoustic sources. In hover, the tip trailing vortex can move upward behind a blade and even pass over the following blade before being swept downward in the rotor wake (Leverton, 1971). The resulting flow incidence changes can cause local blade stall. The effect of local stall on acoustic radiation was studied experimentally for the steady interaction between a stationary blade and an incident trailing vortex by Paterson et al. (1975). However, it is likely that this source is not as important in the forward flight helicopter case where the unsteady stall effects on overall blade forces would probably overshadow the noise associated with any unsteady separated flow.

Noise due to turbulence in blade tip flows can be important at high frequencies as shown by George et al. (1980). Blade tip shapes also affect tip vortex formation, and the resulting trailing edge noise is affected by tip shape modifications.

3.2.7 Noise Due to Turbulent Inflow

An important source of the random part of rotor noise is the fluctuating loading associated with ambient inflow turbulence. Turbulent upwash fluctuations lead to unsteady load fluctuations which radiate sound. Lower frequencies are generated by interactions with larger scale turbulent eddies, and higher frequencies by interaction with smaller eddies. As the larger eddies take a substantial time to be convected through the rotor, the blades interact a number of times with a large eddy leading to a peaked but continuous low frequency part of the spectrum. The incident turbulence may be due to wake re-circulation for helicopters near the ground, ambient atmospheric turbulence, or passage through the turbulent wake of the same or other blades. Also, tail rotors can ingest the turbulent wake of the main rotor causing additional random tail rotor loading and radiation of broadband noise. Signor et al. (1992) experimentally investigate turbulence ingestion for a full scale tail rotor.

Ingested atmospheric turbulence can make a significant contribution to non-impulsive helicopter rotor noise and has been analyzed for isotropic incident turbulence by Homicz and George (1974), Amiet (1977), and George and Kim (1977). The predicted spectra are close to measured hover results although slightly low, possibly due to the neglect of the anisotropicity of the distorted flow. Anisotropic inflow has been experimentally demonstrated by Hanson (1975) for compressor inlets and Pegg et al. (1977) have measured the corresponding reduction of radiated sound for propellers in forward flight. There is still a need for experiments on rotor-turbulence interaction where turbulent flow properties and acoustic data are simultaneously measured.

Simonich et al. (1990) combine several models to describe the fluid mechanics of atmospheric turbulence and the rotor ingestion process. In their method, initially isotropic and locally stationary and homogeneous atmospheric turbulence is distorted by streamline curvature and stream-tube contraction, so the turbulence which arrives at the rotor disk is anisotropic. The turbulence distortions are tracked using rapid distortion theory. A rotor acoustic model and noise predictions based on this technique are presented by Amiet et al. (1990) in a companion paper.

Brooks et al. (1989) identify blade-wake interaction (BWI) as an important rotor broadband noise source, which is due to the ingestion of turbulent portions of the wakes of preceding blades. This source can dominate the mid frequencies of noise spectra during the approach stage of a rotorcraft flyover when BVI noise is not intense. Glegg and Devenport (1991) experimentally study a turbulent tip vortex, and incorporate their results in a turbulence model to predict BWI noise.

3.3 Noise due to T_{ij} Terms

The Lighthill stress term T_{ij}, which is often loosely called the quadrupole term, contains quite a few different mechanisms including nonlinear effects, non-isentropic effects and turbulence. This quadrupole term effect on rotor noise has not been extensively studied until recently. There are several causes for changes in T_{ij} which will contribute to far-field sound. First, analogous to the blade volume case, the geometry (location) of the blade and associated flow field change during the integration of equation (5). This effect might be present even if T_{ij} were constant in blade-fixed coordinates. Calculations of this effect would involve the same sort of complicated geometrical computation as in the blade volume case discussed previously. A second effect is the time variation of T_{ij} in blade-fixed coordinates due to the changing flow field over a rotor blade in forward flight where the relative velocity over the blade can vary cyclically from Mach numbers of say 0.5 to 0.9. As the blade passes in and out of supercritical flow conditions substantial flow changes such as the formation and decay of shocks occur (Tijdeman, 1977). A third cause of T_{ij} variations can be flow changes due to the passage of a blade near or through a trailing vortex. Tangler (1977) has shown that this passage can lead to rapid and substantial flow changes and shock formation.

The $\rho u_i u_j$ term in Lighthill's stress tensor can be further decomposed by substituting $u_i = U_i + v_i$, where U_i is the mean but possible unsteady flow and v_i is associated with turbulence. Then $\rho u_i u_j$ becomes $\rho U_i U_j + \rho(U_i v_j + U_j v_i) + \rho v_i v_j$. The last term represents the quadrupole source effects due to turbulence while the second term originates in the interaction between the mean flow and turbulent velocities. This second term is only important for transonic blade speeds and it seems unlikely to be as important as non-turbulent effects for high tip speed helicopter rotors.

The unsteady mean flow effect seems to be important for helicopter rotors. This $\rho U_i U_j$ term and the $(p - c_o^2 \rho)$ also in T_{ij} include what are traditionally thought of as transonic flow effects such as shock waves and high local flow velocities. Kitaplioglu and George (1977) first considered the far-field radiation from a model of instantaneous shock formation and disappearance. Their order of magnitude estimates showed that for instantaneous flow changes the steep gradients associated with shock waves are more important than the more gradual flow gradients elsewhere on the blade. But if time variations are more gradual, overall changes in T_{ij} are important regardless of whether they occur in thin or discontinuous regions, such as shocks, or whether they are spread out in the flow around the blade. Schmitz and Yu (1979) discovered that acoustic disturbances accumulate to form a local shock on the blade surface which eventually becomes a radiating shock wave as the advancing tip Mach number increases. This "shock delocalization" process can be successfully modeled with the inclusion of quadrupole terms (Splettstoesser et al., 1983 and Schmitz and Yu, 1986). Farassat and Succi (1983) highlighted the need to include these shock formation and quadrupole noise effects for thickness noise calculations at high tip Mach number. More recently, Farassat (1987) showed that Lighthill's quadrupole term can be effectively decomposed into a pure quadrupole term, a blade surface term, a shock surface term and a trailing edge term. Away from the boundary layers, wakes and vortices, the pure quadrupole sources are very inefficient noise generators and their basic function is to correct for variation in sound speed near the blade and the finite fluid particle velocity there. The blade surface and shock terms act effectively as dipole sources, while the trailing edge term is more appropriately modeled as a monopole term. These results are part of the work actively being pursued on high-speed impulsive (HSI) noise research and is summarized in Schmitz (1991).

4.0 RECENT PROGRESS IN TILT ROTOR NOISE

This section will report some recent progress made at Cornell University in understanding and predicting two important tilt rotor noise mechanisms. The tilt rotor fountain effect will be covered in Section 4.1, then blade-vortex interaction noise is addressed in Section 4.2.

4.1 Tilt Rotor Fountain Effect

During the operation of a tilt rotor aircraft in hover, the presence of the wing and fuselage beneath the rotor affects the aerodynamics by introducing complex unsteady recirculating flows. Figure 3 shows a schematic sketch of the resulting flow. The wing and fuselage provide a partial ground plane which causes an inboard-bound spanwise flow over the wing and fuselage surface. At the aircraft's longitudinal plane of symmetry, the opposing flows collide, producing an unsteady "fountain flow" with upward velocity components. This fountain flow is then re-ingested by the rotors. The interaction of the rotors with these complex flows results in significant noise radiation. To predict such noise, the recirculating flows must be understood, and then appropriately modeled.

There is ongoing research at Cornell to understand and predict the flow field and noise of a tilt rotor in hover. This work is a blend of computation and experiment. Our experimental approach involves flow visualization and hot wire anemometry to help understand and model features of the recirculating fountain flow, and acoustic measurements to help understand the influence of these effects on rotor noise radiation. In addition, the acoustic prediction program WOPWOP is used to compute the noise radiated from these sources. Some recent progress in this research will be discussed in the following three sections.

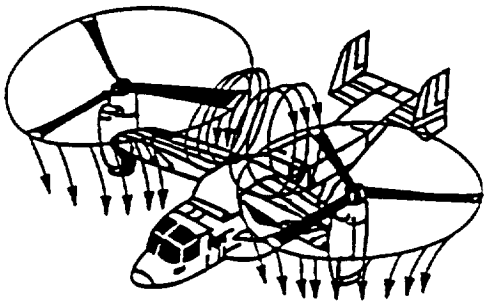

Figure 3. Flow field of a tilt rotor in hover showing recirculating fountain flow.

4.1.1 Model Dimensional Analysis

Some characteristics of full-scale, and nearly full-scale, tilt rotor hover aerodynamics have been studied experimentally by Felker et al. (1986), Felker and Light (1988), and Felker (1992). Also, results from smaller-scale models have been reported by Norman and Light (1987), McVeigh et al. (1990), and Coffen et al. (1991). There are several advantages to the small-scale model approach to this problem, including low cost, ease of instrumentation, and ease of testing aircraft configuration changes. In addition, most large scale tests have used a single rotor and wing combination, invoking a symmetry assumption along the aircraft's longitudinal plane. While this boundary condition is nearly correct for time-averaged measurements, it does not simulate the three-dimensional, unsteady aspects of the fountain flow, which are important to noise radiation. These features are best studied on a model which includes both rotors. In particular, to assess the aeroacoustic effects of configuration changes, an image-plane model should not be used.

Figure 4 shows Cornell's 0.08 scale model of the XV-15. Two uncoupled electric motors are rigidly bolted to steel frames, and power commercial two-bladed model airplane propellers. The model rotor speeds are matched using a stroboscope. While different propellers can be used on the model, the ones chosen for all the results discussed here operate at a thrust coefficient, $C_T = T/\rho A V_{tip}^2$, of about 0.005, a power coefficient, $Cp = P/\rho A V_{tip}^3$, of about 0.0006, and a figure of merit, $M = T^{3/2}/(2\rho A)^{1/2}$ P, of approximately 0.4. These values are near the low end of full-scale tilt rotor aircraft (Felker et al., 1986). The model blade twist, chord and thickness distributions are similar to the original and ATB XV-15 rotors, except for the unusual thickness distribution of the ATB blade. The model rotor plane is at a scaled altitude of 19.9 m. Also, the model body is bolted to an adjustable stand which allows different rotor plane/wing clearances, and the body can be tilted to simulate tilt-rotor flight for small nacelle angles. The wing flaps and flaperons are fully adjustable.

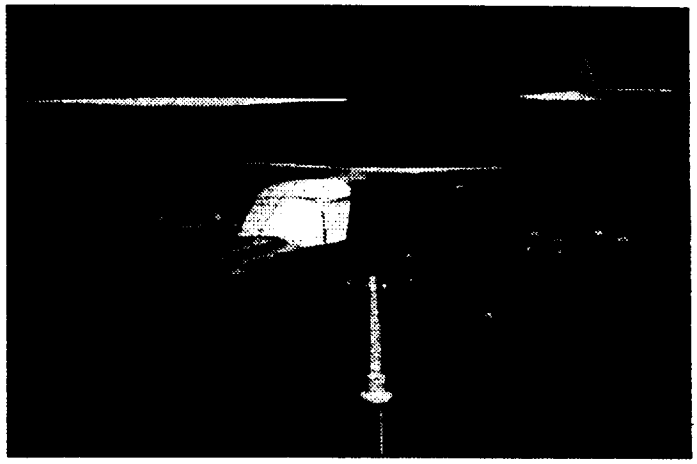

Figure 4. Cornell's 0.08 scale model of the XV-15 in hover.

Table 1 lists some data associated with this model and the full- scale aircraft. The blade tip Mach number and Reynolds number based on V_{tip} are not modeled correctly, but the advance ratio based on mean momentum inflow velocity, and blade solidity are nearly correct in the model scale. For the full-scale, V_{mean} has been estimated from simple momentum theory, debiting 10% for losses, while V_{mean} for the model has been measured by Coffen (1992). Mismatching the tip Mach number affects the acoustic measurements, but it can be approximately accounted for, as discussed below. Also, errors in M_{tip}, R_{tip} and details of the blade geometric distribution are expected to be of secondary importance to the fluid mechanics of the recirculating fountain flow. Finally, the Reynolds number based on V_{mean} is also too low in the model. However, this should have little or no effect on the large-scale turbulence structures which are the prominent feature of the recirculating flow, as will be shown below.

Having established that the model aerodynamics are a good approximation to full-scale, it is necessary to determine length, frequency and velocity scales to relate the model and prototype behavior. Research on twin jet impingement, for example by Miller and Wilson (1993), shows that the important parameters governing these flows are jet radius, jet spacing, clearance from the ground plane, and jet momentum. Although the twin downwash flows induced by a hovering tilt rotor are at much smaller spacings and ground clearances, these results can be used to deduce that the most important parameters governing the fountain flow are geometric similarity and mean inflow velocity. The model is 1/12.5 scale, so $d_m = d_p/12.5$, where d is a characteristic length (rotor diameter), and the subscripts m and p refer to model and prototype, respectively. Also, using mean momentum inflow velocity, the velocity scale from Table 1 is $V_m = V_p/3.3$. Therefore, to satisfy Strouhal similarity, $f_m d_m/V_m$

$= f_p d_p / V_p$, the frequency scale is $f_m = 3.8 f_p$. The model blade passing frequency matches this requirement well, as shown in Table 1.

Along with Reynolds number, the Strouhal number is the most likely similitude parameter characterizing the fountain flow. The Froude number is not expected to be important since there are no free surface or gravitational effects. Also Mach number is not important since the full-scale fountain flow is subsonic. Thus, from this simple analysis, hot wire spectra measured in the fountain flow of the model can be approximated to prototype by dividing frequencies by 3.8, and multiplying velocities by about 3.3.

	XV-15 Prototype	Cornell Model
Tip Mach number, M_{tip}	0.69 0.66 (ATB)	0.33
Blade solidity	0.089 0.103 (ATB)	0.071
$R_{tip} = V_{tip} * d/\nu$	1.2×10^8	4.4×10^6
$R_{mean} = V_{mean} * d/\nu$	8.6×10^6	2.1×10^5
Mean advance ratio $[V_{mean}/(f * d)]$	0.074 - 0.079	0.073
Blade diameter, d	7.62 meters	0.610 meters
Blade passing freq., f	28.3 - 30.2 Hz	115 Hz
Mean inflow vel., V_{mean}	17 m/s	5.1 m/s
Length scale, $[d_m/d_p]$	---	1/12.5
Inflow velocity scale $[V_m/V_p]$	---	1/3.3
Frequency scale, $[f_m/f_p]$	---	3.8

Table 1. Comparison of model and full-scale parameters governing the aerodynamics and aeroacoustics of a tilt rotor in hover.

4.1.2 Experimental Tilt Rotor Hover Aerodynamic Studies

Previous hot wire measurements on the model have been reported by Coffen et al. (1991) and George et al. (1992). Mean and rms velocities measured above the rotor plane clearly showed an inflow velocity defect over the wings, and higher turbulence levels in the fountain reingestion zone. Both of these effects are known to contribute to noise radiation: the velocity defect causes the rotor blades to experience a rapid angle of attack change as they enter and leave this region, and the high turbulence produces unsteady blade pressures. Also, flow visualization using neutrally-buoyant helium-filled soap bubbles clearly demonstrated the existence and unsteadiness of the fountain flow. The fountain height was estimated to be approximately d/4, and only the largest scale eddies were recirculated to the full fountain height. Another important feature identified by this work was the apparent side-to-side shifting of the stagnation area on the model wing upper surface.

Our recent studies have confirmed this unsteadiness in the stagnation zone. Hot wires immersed in the fountain flow below the rotor plane show that most of the velocity fluctuations occur at low frequencies. Low frequency, large-scale turbulence structures are expected in such impingement flows (Kohlman, 1987). TSI single component hot wires were used, along with a TSI Model 1050 Constant Temperature Anemometer, and a Hewlett Packard 3582A Spectrum Analyzer. To measure coherences in the recirculating flow, two hot wires were positioned under the rotor plane at various heights and separation distances. The probes were positioned symmetrically about the model's longitudinal axis, along the line joining the two rotor axes. Coherences of approximately 0.5 to 0.7 were measured between the probes at these locations, at frequencies of about 1.0 Hz, as shown in Figure 5, for example. Sixty-four sample averages were used to generate the spectrum and coherence plots in this figure. The probes were located at the locations shown on the schematic view of the model, 25 mm above the wing surface, with the sensor wires oriented perpendicular to the plane TRNR. To measure such a large coherence at this relatively large probe separation of 178 mm emphasizes the fact that the recirculating flow is composed of regular, large-scale structures.

To investigate this semi-coherent low frequency velocity fluctuation further, a number of 0.12 mm diameter silk threads were attached in a grid to the upper surface of the model wing in the fountain recirculation area. Preliminary results reveal an occasional large-scale side-to-side shifting of the stagnation zone. Also, the lateral velocity is rarely zero along the model longitudinal axis, but continually changes sign as evidenced by the tufts flapping regularly from one side to the other. This provides further evidence that the dynamics of the recirculating fountain flow cannot be captured using a symmetry plane assumption.

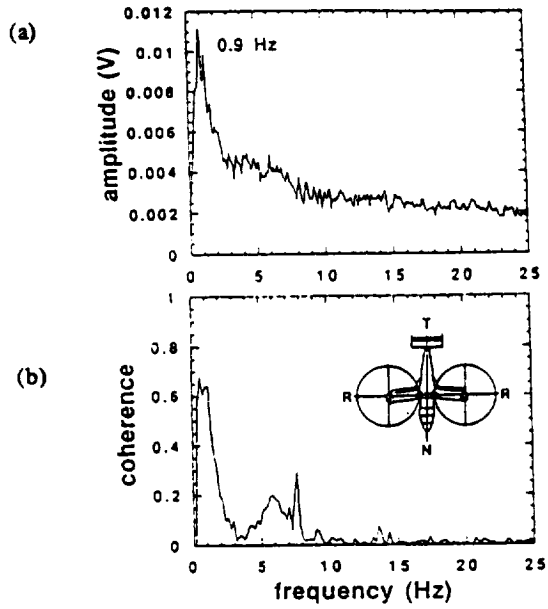

Figure 5. Hot wire amplitude spectrum and coherence of the low frequency velocity fluctuations in the model's recirculating fountain flow.

4.1.3 Experimental Tilt Rotor Hover Acoustic Studies

Acoustic waveforms and time-averaged spectra were also measured from the model. To approximate a free field, the experiments were conducted in the evening in an empty parking lot. The model and microphone were located at least 36 m from the nearest building, so that reflected acoustic waves were much smaller in amplitude than incident waves. A 1/2" General Radio random incidence electret condenser microphone was used along with a windscreen. The microphone was placed on the ground, and was calibrated with a pistonphone before each experiment.

Again, to relate the model experimental results to prototype, scaling laws need to be established. The frequency scale is known. To estimate the acoustic pressure scale, use is made of Farassat's formulation (1A) (Brentner, 1986). For far field loading noise,

$$4\pi\, p(\underline{x},t) = \frac{1}{c} \int_{f=0} \left[\frac{\dot{l}_i\, \hat{r}_i}{r\,(1 - M_r)^2} \right]_{ret} ds \qquad (6)$$

where the integration is performed over the blade surface, defined by the function f=0. Also, r is the source-observer propagation distance, M_r the blade element Mach number in the observer

direction, and $\dot{l}_i$ is the time derivative of the force per unit area on the fluid. By the Mean Value Theorem, equation (6) can be replaced by the mean value of the integrand multiplied by the total blade surface area. Since estimating the mean value is very difficult, instead the integrand is replaced by characteristic values, and the ratio p_p/p_m is considered:

$$\frac{p_p}{p_m} = \left(\frac{\sigma_p}{\sigma_m}\right)\left(\frac{d_p}{d_m}\right)^2\left(\frac{r_m}{r_p}\right)\left(\frac{1-M_{tipm}}{1-M_{tipp}}\right)^2\left(\frac{\dot{l}_{ip}}{\dot{l}_{im}}\right) \qquad (7)$$

The term $\dot{l}_{ip}/\dot{l}_{im}$ can be estimated using linearized aerodynamics.

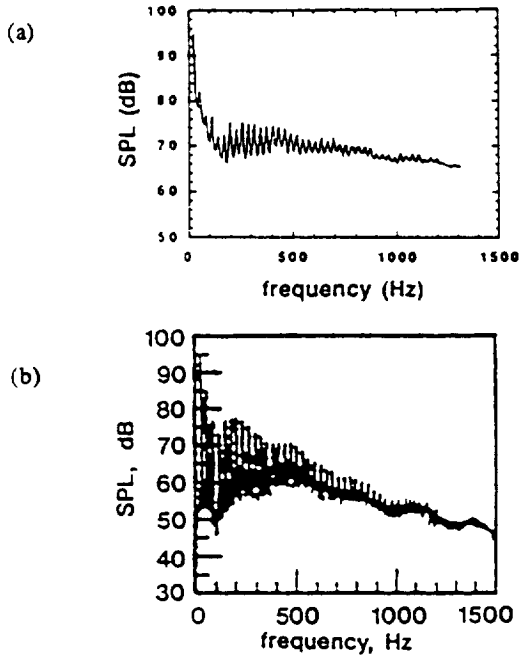

Figure 6. Comparison of (a) scaled -model acoustic spectrum (present research), and (b) full-scale XV-15 acoustic spectrum (from Conner and Wellman, 1991).

As an example, Figure 6 compares a scaled-model and full-scale acoustic spectrum. This case is for r = 218 m, directly to the rear of the aircraft, approximately 7 degrees below the rotor disk plane. Equation (7) estimates a model correction of +35 dB for both the fountain turbulence and velocity-defect noise mechanisms, which is close to the correction applied in Figure 6 of +30 dB. The +30 dB correction was established by matching the amplitudes of the blade passing frequency. The difference between the estimated and actual spectrum correction is relatively small considering the level of approximation in equation (7), and the fact that full-scale and model-scale experimental uncertainty is on the order of ±1.5 dB (Conner and Wellman, 1991). Applying a similar analysis as used to derive equation (7), the corrections for atmospheric turbulence ingestion and thickness noise are approximately +46 and +36 dB, respectively, for this case. Thus, the model tends to amplify the two aeroacoustic sources related to the fountain effect, which is favorable since these are the effects being studied.

There are some differences in the spectra shown in Figure 6, for instance the scaled-model levels are higher for frequencies larger than about 800 Hz. Also, the peak-valley separation of the scaled-model spectrum is not as large as full-scale. However, the amplitudes of the first 20 or so harmonics of the blade passing frequency agree relatively well between model and prototype, which is most important.

Figure 7 compares model- and full-scale waveforms for the case of r = 218 (m), directly behind the aircraft. For the model, the angle below the rotor disk, θ, is about 18 degrees, which is compared to the closest available full-scale data of θ=12.6 and θ=23.0 degrees. Equation (7) estimates a correction of about +25 dB, while that shown in Figure 7 is +17.5 dB, which do not agree as well as for the previous case. Again, the +17.5 dB was established by matching the amplitudes of the fundamental blade passing frequency. Figure 7 shows that the most important features of the prototype acoustic waveform are reproduced in model scale. Note the impulsive part of both the model and prototype waveforms which is caused by the inflow velocity defect discussed earlier.

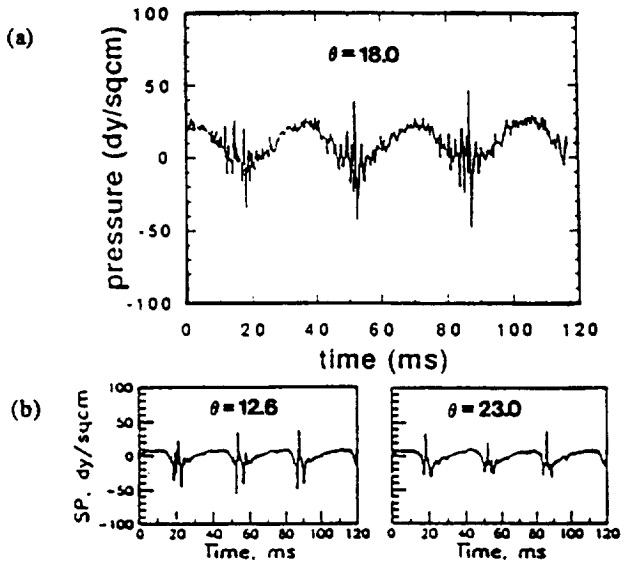

Figure 7. Comparison of (a) scaled-model acoustic waveforms (present research), and (b) full-scale XV-15 acoustic waveforms (from Conner and Wellman, 1991).

4.1.4 Computational Tilt Rotor Hover Acoustics Studies

Discrete hover noise calculations by Rutledge et al. (1991) using WOPWOP incorporated a simple model for the inflow velocity defect, which was based on measurements taken on the model. Good agreement was obtained with experiment both in the acoustic level and directivity. The results also showed that the velocity defect caused the impulsive feature in the observed acoustic waveforms, providing further evidence that the fountain effect is a dominant noise mechanism for hovering tilt rotors.

Broadband noise predictions were reported by George et al. (1992). They used a modified method of Amiet (1989) to account for azimuthally and radially varying turbulence levels, as scaled from measurements made on the model. The predictions were within about 3 dB of experiment, and show that the high broadband levels for tilt rotors in hover can also be explained by the fountain recirculation.

4.2 Blade-Vortex Interaction (BVI) Noise

As discussed previously in this paper, blade-vortex interaction noise is a major tilt rotor problem. Although severe BVI occurs only over a portion of the tilt rotor or helicopter operational envelope, when BVI does occur, it is highly directional and dominates the acoustic pressure field.

Our recent work primarily treats the directionality of BVI noise radiation. Subsonic BVI noise radiation can be considered as composed of two main mechanisms: an unsteady net force effect and the radiation cone effect. However, our recent findings have indicated that the unsteady velocity effect can be important as well. By understanding the directionality of BVI acoustic mechanisms it can be better insured that acoustic energy is not directed towards particularly sensitive areas or buildings. It is

possible to control the directionality of acoustic radiation by a wise choice of operating conditions. The tilt rotor flight envelope allows a range of RPM/flap angle/nacelle angle combinations to satisfy a single flight condition, (George et al, 1989). A proper choice of this combination could perhaps yield large reductions in BVI sound radiation or change in directionality at a minimal cost. The purpose of our study is to show that the directionality of blade vortex interactions can be quite well predicted by relating it to the blade-vortex intersection sources. A careful investigation of the BVI parameters at these source locations yields a better concept of how BVI noise is radiated and possible noise reduction strategies.

4.2.1 Fundamental Mechanisms

The important sources of acoustic radiation emitted from blade-vortex interactions can be classified into two categories; unsteady net force radiation and Mach cone radiation. The unsteady net force radiation is associated with the unsteady lift of the blade surface, while the radiation cone effect is the result of a force distribution moving at a supersonic velocity with respect to the fluid. In addition to the general lift dipole shape, the unsteady net force effect shows only minor directionality effects due to Doppler amplification, while the Mach cone/radiation cone effect will be seen to be highly directional. This mechanism can be identified in the work of Widnall (1971) where it was shown that the component of the blade's Mach number measured along the vortex, known as trace Mach number M_t, was the governing parameter for sound radiation and directivity. For rotating blades, M_t is strongly dependent on the BVI interaction angle γ, rotor's advance ratio μ, normalized blade radial position r_B and azimuth angle φ_B. Ringler et al. (1991) have shown that supersonic trace Mach number can occur in rotor BVI during certain operating conditions where radiated sound energy is focused in preferred directions. A third source of BVI acoustic radiation we have recently discovered is due to caustic effects in radiation. These mechanisms are associated with unsteady velocity changes and source path curvature, and can result in sound waves coalescing in the far-field to form acoustic singularities. Such caustic effects have been investigated by Myers and Farassat (1987) and Sim and George (1993) for high-speed propeller noise, but not for rotor BVI noise before this paper.

4.2.2 Mach Cone/Radiation Cone Concept

This concept can be explained in a similar manner to the classical Mach cone explanation. Each blade segment affected by BVI can be considered as a moving source which generates a signal. The signal emitted from the source moves away from the point of emission at sonic speed. If the sources are moving steadily supersonically, an envelope for each source is formed whose shape is described by the Mach cone. From general Mach cone theory, the wavefront which is produced moves in the direction of $M_r=1$. The direction of M_r equals 1 is equally well described as the normal to a Mach cone surface, referred to as the "radiation cone" in figure 8a. This result implies that this blade vortex interaction noise mechanism is highly directional and that its directionality is predicted primarily by the radiation cone (neglecting unsteady and diffraction effects).

Lowson's equation (Lowson, 1965) for a moving dipole is used to explain the basic mechanisms by Ringler et al. (1991).

$$p(\underline{x},t) \cong \frac{1}{4\pi c r} \sum_{\text{elements}} \left\{ \frac{\sin\theta}{(1-M_r)^2} \left[\frac{\partial F}{\partial t} \right] \right\} \qquad (8)$$

where [ ] denotes evaluation at retarded time, and the Σ corresponds to summing over all the blade elements. This equation can now be broken into a directionality function ($D(\underline{x}) = \sin\theta/(1-M_r)^2$), a geometrical (spherical) decay function ($W(\underline{x}) = 1/4\pi cr$), and a source strength function ($S(\underline{x},t) = \sum_{\text{elements}} [\partial F/\partial t]$). All of these functions are observer position dependent. Even $S(\underline{x},t)$ is a function of space since it is evaluated at the retarded time. Neglecting the effects of diffraction, $S(\underline{x},t)$ can only have two values at any instant in time for steady linear motion; a finite value if the observer is on the radiation cone, and zero for any observer off the radiation cone.

Extensive discussion of results for acoustic radiation from rotating blades undergoing BVI can be found in Ringler et al. (1991). The directionality of blade-vortex interactions was confirmed to be predicted by the radiation cone. High tip velocity usually creates a maximum in the source strength and a supersonic M_t intersection at or near the tip. This maximum source strength coupled with the supersonic M_t makes the radiation emitted near the blade tip much more significant than the radiation which is emitted from inboard locations. Since the blade velocity varies with radial position, the trace Mach number M_t will vary and thus, the directivity as well. Large M_t values radiate acoustic energy nearly perpendicular to the vortex line. At some radial location, M_t will generally equal 1, and the radiation cone is then oriented directly along the vortex line. Thus the movement of the intersection point along the blade can sometimes create changes in directivity on the order of 90°. Therefore in rotating geometries, the direction of acoustic radiation will vary greatly as the intersection point moves along the blade. Generally the most intense signal will result from the high blade Mach number part of the interaction. The importance result is that the direction of maximum acoustic radiation can be found a priori through the Mach/radiation cone concept.

The source strength was found to be remarkably independent of trace Mach number and was essentially the same for all observers on the radiation cone (Ringler et al., 1991). Variation of sound pressure level from point to point on the radiation cone is primarily due to the directivity function, $D(\underline{x})$, which is governed by the dipole radiation and Doppler amplification term.

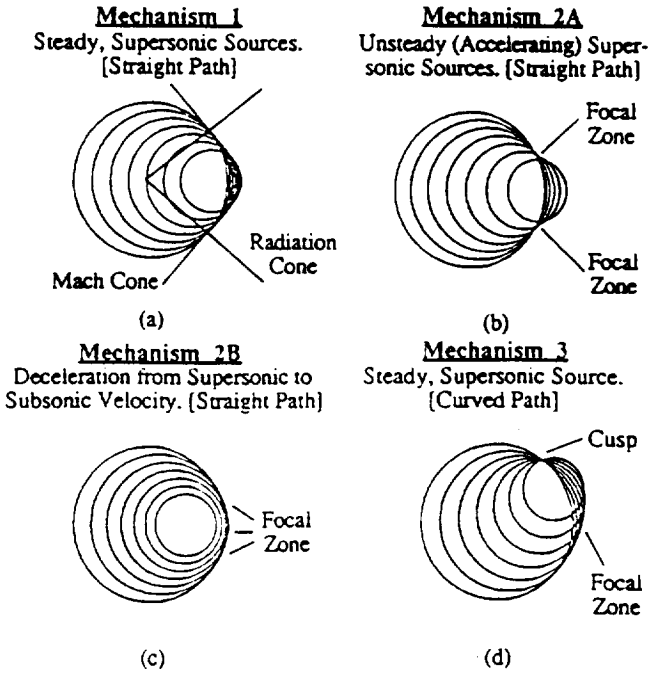

Figure 8. Sound propagation from supersonic sources for different velocity and path settings.

Ringler et al. applied the radiation cone concept to show isolated regions of intense sound pressure levels, often referred to as 'hotspots', observed during XV-15 fly-over tests (Golub et al., 1990). It was determined that at high nacelle angles, the acoustic field was dominated by blade vortex interactions. The results of one test case are shown in figure 9. It is noteworthy that not only was there a hot spot in this test (indicated by point B), but also that the dB level falls off slowly in front of the aircraft. With spherical spreading of the signal it would be expected that the lines of constant dB would be closer together as one moved away from the aircraft. This decay is not seen at all in front of the aircraft in this test case. Therefore, this confirms that highly directional mechanisms produced this signal.

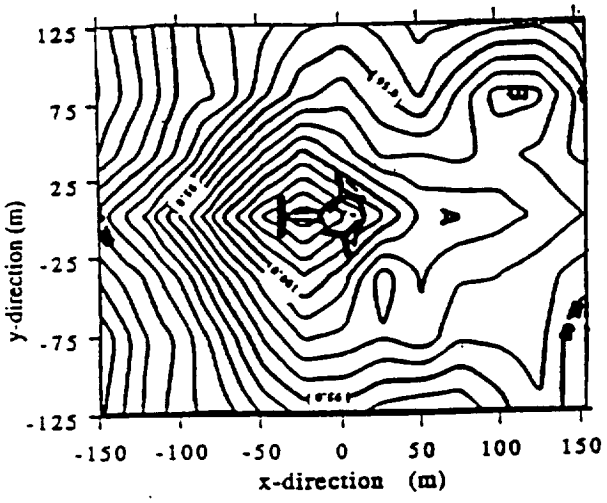

Figure 9. XV-15 experimental results of a level flyover 250 ft above ground plane. [V_B=90 knots, tip-path-plane angle=5°] (from Golub et al., 1990). Hot spots are indicated by "A" and "B".

By using a rigid wake model, Ringler et al. studied the instances where the rotor blade and the tip vortex interact to produce supersonic trace Mach numbers were determined. The intersection of the radiation cones emitted by these sources and the ground plane were found. Figure 10 shows the radiation cones generated by the rotor tip for a three-bladed rotor system (in clockwise rotation) during one blade passing period. A total of five supersonic interactions were found during one blade passing period. Only interaction #1 (advancing side) and #5 (retreating side) correspond to a blade interacting with its own wake. This directivity pattern indicates that the majority of the BVI energy is beamed forward in front of the aircraft. The "hotspots" seen in the experimental results (labeled B in Figure 9) correlates well with directivity prescribed by interaction #1, #3 and #4. Note that #3 has the largest M_t of all the interactions.

4.2.3 Unsteady Velocity and Source Path Effect

Acoustic wave propagation is known to exhibit different far-field behaviors under various conditions. These behaviors can be caused by source acceleration or deceleration, curvature in path geometry or diffraction effects. It was shown that a Mach cone/radiation cone is formed as a result of steady supersonic BVI sources traveling on a straight trajectory (Mechanism 1) shown in figure 8a. The Mach cone carries a substantially higher noise disturbance as a result of multiple acoustic waves arriving at the same time. An extension to this effect is to look at the acoustic propagation when the velocity is unsteady (Mechanism 2A and 2B) and when the source path is curved (Mechanism 3). Figure 8a, 8b, 8c and 8d illustrate the effect of these mechanisms on far-field sound propagation. It is found that a combination of these factors can lead to focused sound waves known as caustics. Location of these caustics are critically dependent on the velocity of the source and path curvature. Studies of such acoustic phenomenon have been performed by Wanner et al. (1972) and Plotkin and Cantril (1976) for sonic boom evaluations.

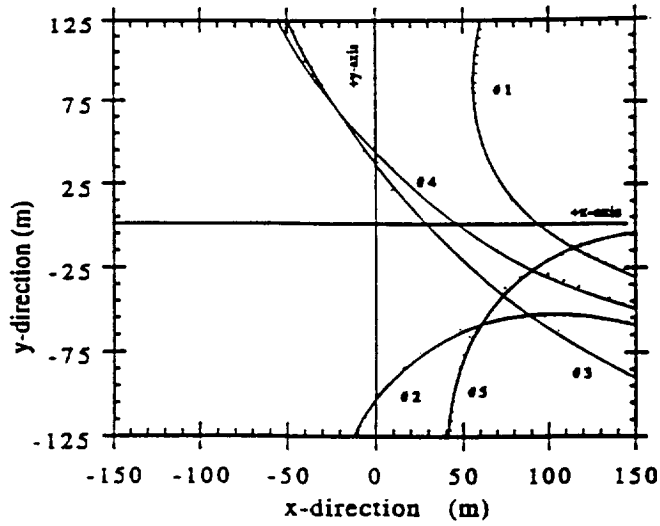

Figure 10. Intersection of radiation cones with ground plane for a three-bladed rotor (from Ringler et al., 1991), at the same condition as figure 9 on the starborad side.

BVI noise sources can be isolated by tracing their interaction geometry along the rotating blade. These sources can be treated as sources (with varying strength) traveling along the blade-vortex intersection trajectory at some trace Mach number. For rotating blades, these sources typically have: (1) unsteady trace Mach number, and (2) source path curvature following the vortex trajectory. Source path curvature is simply a function of the vortex geometry, advance ratio and blade azimuthal angle for a rigid wake model. Figure 11 shows the BVI source locus for a single-bladed rotor with advance ratio of 0.196 at 5° blade rotation azimuth increments. The rotor wake is assumed to be rigid and trails from the tip. The blade azimuth angle and trace Mach number corresponding to each source after 1 complete blade revolution is presented in Table 2. Two distinct regions of BVI noise sources can be observed: advancing side (A1-A11) and retreating side (R1-R10) of the rotor. Both sets of BVI have supersonic M_t at some source positions. Trace Mach number on retreating side BVI decreases rapidly from a supersonic to a subsonic value and increases again later. The advancing side BVI tends not to show the same behavior and M_t is always decreasing but at a slower rate than the retreating side BVI.

	ADVANCING			RETREATING	
	φ_B	M_t		φ_B	M_t
A1	60.0°	1.461	*R1*	325°	1.076
A2	65.0°	1.383	*R2*	330°	0.761
A3	70.0°	1.289	*R3*	335°	0.632
A4	75.0°	1.175	*R4*	340°	0.570
A5	80.0°	1.043	*R5*	345°	0.544
A6	85.0°	0.894	*R6*	350°	0.541
A7	90.0°	0.739	*R7*	355°	0.559
A8	95.0°	0.589	*R8*	360°	0.600
A9	100.0°	0.457	*R9*	365°	0.669
A10	105.0°	0.348	*R10*	370°	0.780
A11	110.0°	0.262			

Table 2. BVI source locations and corresponding trace Mach numbers for a one-bladed rotor after one revolution. Rotor nacelle angle is 85° and advance ratio is 0.196. (Max. M_t=1.475 @ 59° [Advancing], Max. M_t=1.483 @ 22.5° [Retreating]).

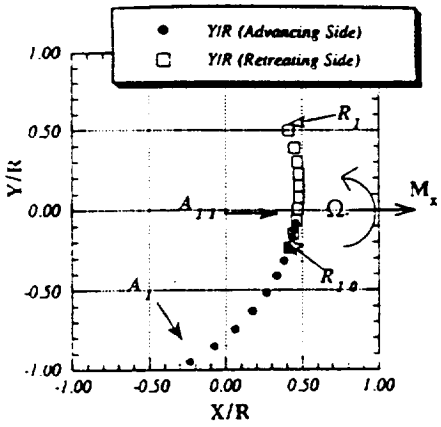

Figure 11. Location of BVI sources for a single-bladed rotor in a blade-fixed coordinate. [μ=0.196, V_B=86.8 knots, tip-path-plane angle=5°]. The sources' trace Mach number are given in table 2.

Based on the calculated BVI source locus and trace Mach number, it is found that caustics are formed in the rotor sound field due to Mechanisms 1, 2B or 3. Mechanism 2A is not significant because no BVI sources are accelerating at supersonic M_t. Figure 12 shows the position of BVI source-generated sound waves in the rotor disc plane after one complete blade revolution for both advancing and retreating side BVI. Of primary interest to us is the directivity of the advancing side interactions because they have generally higher intensity than the retreating side interactions. BVI sources with supersonic M_t are observed between blade azimuth angle ranging from 60° to 80°. Acoustic directivity from these sources can be attributed to Mechanism 1. The radiation cones generate symmetrical "hotspots" indicated by location (I) and (II) forward of the rotor on figure 12. These "hotspots" account for the slow acoustic decay forward-halve of the rotor as shown in figure 9. Positions of these radiation cone-generated "hotspots" are traced by interaction #1 on figure 10. Effects of unsteady velocity also project intense acoustic disturbances at location (III) in front of the rotor. This hot spot can be explained by Mechanism 2B and is due to the deceleration effects of the BVI sources from supersonic to subsonic M_t. Although the BVI parameters are not identical, the emergence of (III) in the rotor disc-plane corresponds with "hotspot" B observed on figure 9 for ground observers.

Acoustic radiation from the retreating side BVI exhibits sound focusing effects at location (IV). This is also due to the effect of decelerating M_t from supersonic to subsonic state associated with Mechanism 2B. The hot spot generated by retreating side BVI corresponds with the region of high intensity occurring at the rotor sides on figure 9 and is represented by interaction #5 on figure 10. It is also noticed that a region of converging sound waves can be seen at location (IV) due to accelerating (subsonic) trace Mach numbers. However, they do not result in caustic generation.

Wave focusing effect due to Mechanism 3 is not significant for this rotor case. This is due to the relatively straight trajectory the supersonic M_t sources are distributed at high advance ratio. However, it is speculated that this mechanism will gain importance for low advance ratio flight conditions where the vortex trajectories have more curvature.

5.0 NOISE REDUCTION TECHNIQUES

A new surge of interest in rotor acoustics, partly inspired by the NASA/AHS National Rotorcraft Noise Reduction Program, has spawned many efforts to quieting V/STOL aircraft (Childress, 1991). This has increased understanding of many noise mechanisms. It is recognized that noise reduction is closely related to noise prediction. As we have seen, a variety of sources can be of practical importance for helicopters and we need to know which ones are dominant and how they depend upon design and operating parameters in order to be able to reduce them.

The velocity dependence of all rotor noise mechanisms is very strong and as a result a primary noise reduction technique is a reduction in rotor tip speed. This reduces rotational noise due to slower source motion, reduces random noise by reducing loadings due to velocity fluctuations, and reduces high Mach number effects by reducing advancing blade Mach number. However, tip speed reduction is limited by adverse effects on helicopter performance and an autorotative capability. Other general noise reduction techniques involve reduced disc loading, changes in blade number and blade geometry. However, some of these parameters can have opposite effects on different mechanisms. For example, an increased number of identical blades can increase turbulent inflow noise (George, 1974) but reduce and raise the frequencies of the rotational noise. Thus, trade-offs must be made based on knowledge of which noise mechanisms are dominant for the particular rotorcraft.

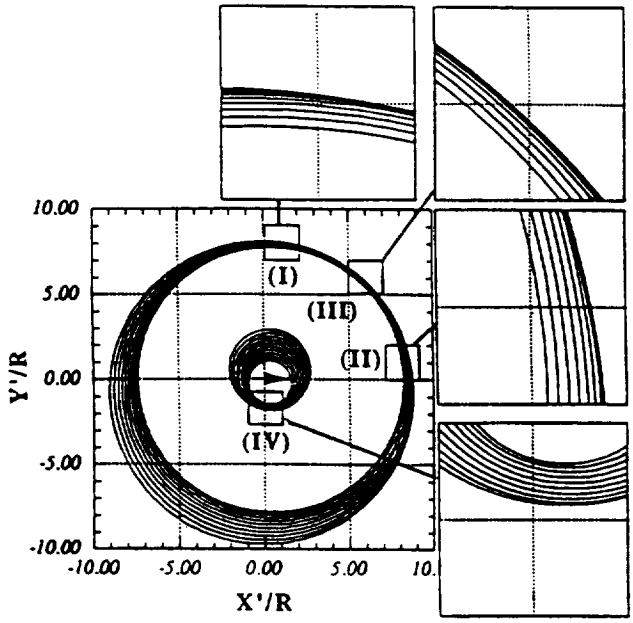

Figure 12. In-plane sound propagation from BVI sources illustrated in figure 11 after one blade revolution. Advancing side BVI noise is propagated further than retreating side BVI noise. "Hotspots" are marked by (I), (II), (III) and (IV).

In particular, designing rotors to minimize BVI noise has been challenging. It has been realized that BVI noise can be affected noticeably by design changes. Hardin and Lamkin (1986) have identified four main parameters, (incoming vortex strength, blade lift, blade curvature and vortex-blade miss distance), that are plausible subjects of control for BVI noise reduction. In addition we have shown that BVI trace Mach number and its variation is important. Airfoil shape is also known to affect transonic BVI (Lyrintzis, 1991). Another approach is to modify the rotor tip region in such a way as to diffuse the tip's trailing vortex and hence reduce the impulsive forces and sound (Schmitz, 1991). Techniques investigated include Tip Air Mass Injection (TAMI) system, spoilers, taper tips, split tips, ogee tips, subwings etc. (Mantay et al., 1977 and Hoad, 1979). Recent studies by Lee (1993) have suggested possible far-field noise reduction using a porous leading edge. Brooks (1993) has shown promising results for a Variable Impedance/Resonance blade and a forward swept planform blade. Another viable method for minimizing BVI noise is Higher Harmonic Control (HHC). Brooks et al. (1990) and Splettstoesser et al. (1990) have demonstrated that a suitably phased input of higher harmonic excitation through cyclic pitch control can cause a reduction in BVI noise. Such a system allows control of the blade angle of attack, and thus its lift and trailed

vortex strength, at any azimuth angle throughout blade rotation. However, in spite of all this past research, it is still difficult to obtain large reductions in BVI noise, except by reduced tip speed and the use of a larger number of blades which makes the BVI noise weaker but more frequent.

6.0 CONCLUSIONS

As we have seen, helicopter noise research is making progress. Knowledge of basic source mechanisms which control rotor noise is growing, although it is far from complete.

For tilt rotors in hover, significant progress has been made in understanding and predicting the aerodynamics and aeroacoustics related to the rotor/airframe interference. At Cornell, important parameters describing the rotor/airframe interaction flows have been identified, and scaling laws have been developed to relate our scale model measurements to prototype. Our measurements have shown that the fountain flow is three-dimensional, unsteady, and highly turbulent. This flow is characterized by large scale, low frequency, semi-coherent velocity fluctuations. Some results from these experimental studies have been successfully used to calculate noise caused by (1) the velocity defect over the aircraft's wings and (2) the high turbulence levels in the fountain reingestion zone. These acoustic features are also reproduced reasonably well in our experimental model. Some future work will include evaluating the aeroacoustic effects of configuration changes on the model, and developing more detailed aerodynamic models for noise prediction.

In addition, our BVI study at Cornell has identified three mechanisms that affect BVI noise directivity. These mechanisms are: (1) the radiation cone effect due to supersonic trace Mach number, (2) the unsteady trace Mach number effect and (3) the path curvature effect. (Only the first two were shown in our sample case.) A supersonic trace Mach number (and its rate of change) seems to be the most important factor governing BVI noise directivity. Future developments will include extending our current understanding for out-of-plane noise and multiple-bladed rotors. A prescribed wake model is also under development to compliment these BVI noise predictions.

7.0 ACKNOWLEDGEMENTS

This research was supported by NASA Ames Grant NAG-2-554 and by NASA Langley Contract NAG-1-1396. The assistance of Todd Ringler and undergraduate researchers, Jaime Estupinan and Alec Stevens, are gratefully acknowledged.

REFERENCES

Amiet, R.K., Simonich, J.C., and Schlinker, R.H., "Rotor Noise Due to Atmospheric Turbulence Ingestion-Part II: Aeroacoustic Reults", *J. Aircraft*, Vol. 27, No. 1,pp. 15-22, January 1990.

Amiet, R.K., "Noise Produced by a Turbulent Flow Into a Rotor: Theory Manual for Noise Calculation," NASA Contractor Report 181788, 1989.

Amiet, R. K., "Noise Produced by Turbulent Flow into a Propeller or Helicopter Rotor," *AIAA Journal*, Vol.15, pp. 307-308, 1977.

Amiet, R. K., "Noise due to Turbulent Flow Past a Trailing Edge," *J. Sound and Vibration*, Vol. 47, pp. 387-393, 1976.

Beddoes, T. S., "A Wake Model for High Resolution Airloads," International Conference on Rotorcraft Basic Research, North Carolina, Feb. 19-21, 1985.

Bliss, D. B. and Miller, W. O., "Efficient Free Wake Calculations Using Analytical/Numerical Matching and Far-Field Linearization," Presented at the 45th Annual Forum of the AHS, Boston, MA, May 1989.

Brentner, K. S. and Farassat, F., "Helicopter Noise Prediction: The Current Status and Future Direction," Proceedings of DGLR/AIAA 14th Aeroacoustics Conference, Aachen, Germany, May 11-14, 1992.

Brentner, K. S., "Prediction of Helicopter Rotor Discrete Frequency Noise: A Computer Program Incorporating Realistic Blade Motions and Advanced Acoustic Formulation," NASA Technical Memorandum 87721, 1986.

Brooks, T. F., "Studies of Blade-Vortex Interaction Noise Reduction by Rotor Blade Modification," Proceedings of Noise-Con 93, Williamsburg, Virginia, May 1993.

Brooks, T. F., Booth, E. R., Jolly, Jr. J. R., Yeager W. T. and Wilbur, M. L., "Reduction of Blade-Vortex Interaction Noise through Higher Harmonic Pitch Control," *J. Am. Helicopter Soc.*, pp. 86-91, 1990.

Brooks, T. F., Marcolini, M. A., and Pope, D. S., "Main Rotor Broadband Noise Study in the DNW", *J. Am. Helicopter Soc.*, pp. 3-12, April 1989.

Brooks, T. F. and Schlinker, R. H., "Progress in Rotor Bradband Noise Research," *Vertica*, Vol. 7, No. 4, pp. 287-307, 1983.

Burley, C. L. and Martin, R. M., "Tip-Path-Plane Angle Effects on Rotor Blade-Vortex Interaction Noise Levels and Directivity," Presented at the 44th Annual Forum of the AHS, Washington, D.C., June 1988.

Chase, D. M., "Sound Radiated by Turbulent Flow Off a Rigid half Plane as Obtained from a Wavevector Spectrum of Hydrodynamic Pressure," *J. Acoust. Soc. Am.*, Vol. 52, pp. 1011-1023, 1972.

Childress, O. S., Jr., "The NASA/AHS Noise Reduction Program - A Brief Overview," Presented at the 1991 NATO CCMS Symposium on Noise Aspects of Rotary-Wing Aircraft, July 1991.

Coffen, C.D., "Tilt rotor Hover Aeroacoustics," Master's Thesis, Department of Mechanical and Aerospace Engineering, Cornell University, 1992.

Coffen, C. D., George, A. R., Hardinge, H., and Stevenson, R., "Flow Visualization and Flow Field Measurements of a 1/12 Scale Tilt Rotor Aircraft in Hover," Proceedings of the AHS Technical Specialists' Meeting. October, 1991.

Conner, David A., and Wellman, Brent, "Far-Field Hover Acoustic Characteristics of the XV-15 Tiltrotor Aircraft with Advanced Technology Blades", AHS/RAeS Technical Specialists Meeting on Rotorcraft Acoustics and Fluid Dynamics, October 15-16, Philadelphia, Pa. 1991.

Cox, C. R., "Helicopter Rotor Aerodynamic and Aeroacoustic Environments", AIAA Paper No. 77-1388, 1977.

Deming, A.F., "Noise From Propellers with Symmetrical Sections of Zero Blade Angle, II", NACA TN-679, 1938.

Dunn, M. H., and Farassat, F., "State-of-the-Art of High-Speed Propeller Noise Prediction - A Multidisciplinary Approach and Comparison with Measured Data," AIAA Paper No. 90-3934, 1990.

Egolf, T. A. and Landgrebe, A. J., "Helicopter Rotor Wake Geometry and Its Influence in Forward Flight, Volume I - Generalized Wake Geometry and Wake Effect on Rotor Airloads and Performance," NASA CR-3726, 1983.

Farassat, F., Lee, Y.-J., Tadghighi, H. and Holz, R., "High-Speed Helicopter Rotor Noise-Shock Waves as a Potent Source of Sound," Unsteady Aerodynamics, Aeroacoustics and Aeroelasticity of Turbomachineries and Propellers, edited by H. M. Atassi, pp. 655-668, Sept. 1991.

Farassat, F., "Quadrupole Source in Prediction of the Noise of Rotating Blade - A New Source Description," AIAA Paper No. 87-2675, October 1987.

Farassat, F. and Succi, G. P., "The Prediction of Helicopter Rotor Discrete Frequency Noise," *Vertica*, 7(4), 1983.

Farassat, F., "Theory of Noise Generation from Moving Bodies with an Application to Helicopter Rotors", NASA TR R-451, Dec. 1975.

Felker, F. F., "Wing Download Reults from a Test of a 0.658-Scale V-22 Rotor and Wing", *J. Am. Helicopter Soc.*, pp. 58-63, October 1992.

Felker, F. F., and Light, J. S., "Aerodynamic Interactions Between a Rotor and Wing in Hover", *J. Am. Helicopter Soc.*, pp. 53-61, April 1988.

Felker, F. F., Maisel, M. D., and Betzina, M. D., "Full-Scale Tilt-Rotor Hover Performance", *J. Am. Helicopter Soc.*, pp. 10-18 April 1986.

Ffowcs Williams, J. E. and Hall, L. H., "Aerodynamic Sound generation by Turbulent Flow in the Vicinity of a Scattering half Plane," *J. Fluid Mechanics*, Vol. 40, pt. 4, pp. 657-670, 1970.

Ffwocs Williams, J. E. and Hawkings, D. L., "Sound Generation by Turbulence and Surfaces in Arbiturary Motion," *Phil. Trans. Royal Society of London*, A264, pp. 321-342, 1969.

Filotas, L. T., "Vortex Induced Helicopter Blade Loads and Noise," *J. Sound and Vibration*, Vol. 27, pp. 387-398, 1973.

Gallman, J. M., "The Validation and Application of a Rotor Acoustic Prediction Computer Program," U.S. Army Aeroflightdynamics Directorate Report No. AD-A222 725, 1990.

George, A. R., Coffen, C. D. and Ringler, T. D., "Advances in Tilt Rotor Noise Prediction," Proceedings of the DGLR/AIAA 14th Aeroacoustics Meeting, Aachen, Germany, May 11-14, 1992.

George, A. R., Smith, C. A., Maisel, M. D., and Brieger, J. T., "Tilt Rotor Aircraft Aeroacoustics," Proceedings of the 45th Annual Forum of the AHS, Boston, MA, May 22-24, 1989.

George, A. R. and Chou, S.-T., "A Comparitive Study of Tail Rotor Noise Mechanisms," *J. Am. Helicopter Soc.*, pp.36-42, 1986.

George, A. R. and Chang, S.-B., "Flow Field and Acoustics of Two-Dimensional Transonic Blade-Vortex Interactions," AIAA Paper No. 84-2309, 1984.

George, A.R., Najjar, F.E., and Kim, Y.N., "Noise Due to Tip Vortex Formation on Lifting Rotors," AIAA Paper 80-1010, 1980.

George, A.R., "Helicopter Noise: State-of-the-Art," *J. Aircraft*, Vol. 15, No. 11, pp. 707-715, November 1978.

George, A.R., and Kim, Y.N., "High-Frequency Broadband Rotor Noise," *AIAA Journal*, Vol. 15, pp. 538-545, April 1977.

George, A. R., Homicz, G. F., Kim, Y. N., Kitaplioglu, C., Pien, W. S., and Sears, W. R., "Research on Helicopter Rotor Noise," Proceedings of the Second Interagency Symposium of University Research in Transportation Noise, North Carolina State University, Rayleigh, North Carolina, pp. 328-345, June 1974.

Ghee, T. A. and Elliot, J. W., "A Study of the Rotor Wake of a Small-Scale Rotor Model in Forward Flight Using Laser Light Sheet Flow Visualization with Comparisons to Analytical Models," Presented at the Annual Forum of the AHS, Washington, D.C., June 3-5, 1992.

Glegg, S., and Devenport, W. J., "The Application of Experimental Data to Blade Wake Interaction Noise Prediction," Unsteady Aerodynamics, Aeroacoustics and Aeroelasticity of Turbomachines and Propellers, ed. by H.M. Atassi, September, 1991.

Golub, R.A, Becker, L.E., Rutledge, C.K., Rita, A.S., and Conner, D.A., "Some Far-Field Acoustics Characteristics of the XV-15 Tilt-Rotor Aircraft," AIAA Paper No. 90-3971, 1990.

Gutin, L. Y., "On the Sound Field of a Rotating Propeller," NACA TM-1195 (1948). Translated from *Phys. Zeit. Sowjet*, Band A, pp. 57-71, 1936.

Hanson, D. B., "Measurements of Static Inlet Turbulence," AIAA Paper No. 75-467, March 1975.

Hardin, J. C. and Lamkin, S. L., "Concepts for Reduction of Blade-Vortex Interaction Noise," AIAA Paper No. 86-1855, 1986.

Hassan, A. A. and Charles, B. D., "Simulation of Realistic Rotor Blade-Vortex Interactions Using a Finite-Difference Technique," AIAA Paper No. 89-1847, 1989.

Hawkings, D. L., and Lowson, M. V., "Theory of Open Supersonic Rotor Noise," *J. Sound and Vibration*, Vol. 36, No. 1, 1974.

Hoad, D. R., "Evaluation of Helicopter Noise due to Blade-Vortex Interaction for Five Tip Configurations," NASA TP-1608, December 1979.

Hoffman, J. D. and Velkoff, H. R., "Vortex Flow over Helicopter Rotor Tips," J. Aircraft, Vol. 8, pp. 739-740, Sept. 1971.

Homicz, G. F. and George, A. R., "Broadband and Discrete Frequency Radiation from Subsonic Rotors," *J. Sound and Vibration*, Vol. 36, pp. 151-177, 1974.

Hubbard, H.H., Lansing, D.L., and Runyan, H.L., "A Review of Rotating Blade Noise Technology", *J. Sound and Vibration*, Vol. 19, No. 3, pp. 227-249, 1971.

Johnson, W., "Development of a Comprehensive Analysis for Rotorcraft - I. Rotor Model and Wake Analysis," *Vertica*, Vol.5, pp.99-129, 1981.

Jones, D. S., "Aerodynamic Sound Due to a Source Near a Half Plane," *J. Institute of Mathematics aaand its Applications*, Vol. 9, pp. 114-122, 1972.

Kitaplioglu, C. and George, A. R., "A Study of the Far-Field Sound Due to Unsteady Shocks on Helicopter Rotors," AIAA Paper No. 77-1360, 1977.

Kim, Y.N., and George, A.R., "Trailing-Edge Noise from Hovering Rotors", *AIAA Journal*, Vol. 20, No. 9, pp. 1167-1174, September 1982.

Kohlman, David L., Introduction to V/STOL Airplanes, Iowa State University Press, Ames, 1987.

Lee, D. J., "An Analysis of Blade-Vortex Interaction Aerodynamics and Acoustics," Stanford University, JIAA TR-67, September 1985.

Lee, S., "Effect of Leading Edge Porosity on Blade-Vortex Interaction Noise," AIAA Paper No. 93-0601, 1993.

Lent, H., Lohr, K., Meier, G., Miller, K., Schievelbusch, U., Schurmann, O. and Szumowski, A., "Noise Mechanisms of Transonic Vortex Airfoil Interaction," AIAA Paper No. 90-3972, 1990.

Leverton, J.W., "Twenty-Five Years of Rotorcraft Aeroacoustics: Historical Prospective and Important Issues", *J. Sound and Vibration*, Vol. 133, No. 2, pp. 261-287, 1989.

Leverton, J. W., "Reduction of Helicopter Noise by Use of a Quiet Tail Rotor," *Vertica*, Vol.6, 1982.

Leverton, J. W., "The Sound of Rotorcraft," *The Aeronautical Journal of the Royal Aeronautical Society*, Vol. 75, pp. 385-397, June 1971.

Lighthill, M. J., "On Sound Generated Aerodynamically - I: General Theory," *Proc. Roy. Soc.*, A221, pp. 564-587, 1952.

Lowson, M. V., "Progress Towards Quieter Civil Helicopters", *Aeronautical Journal*, pp. 209-223, 1992.

Lowson, M. V., Byham, G., Perry, F. J. and Hawkings, D. L., "Rotor Tip," British Patent 1539055, US Patent 4077741, etc, 1976.

Lowson, M. V., "Helicopter Noise: Analysis - Prediction and Methods of Reduction," AGARD Report LS-63, 1973.

Lowson, M. V. and Ollerhead, J. B., "A Theoretical Study of Helicopter Rotor Noise," *J. Sound and Vibration*, Vol. 9, pp. 197-222, 1969.

Lowson, M.V., "The Sound Field for Singularities in Motion," *Proc. Roy. Soc.*, A286, 559-72, 1965.

Lyrintzis, A. S. and Xue, Y., "Study of the Noise Mechanisms of Transonic Blade-Vortex Interactions," *AIAA Journal*, Vol. 29, No. 10, pp. 1562-1572, 1991.

Lyrintzis, A. S. and George, A. R., "Far-Field Noise of Transonic Blade-Vortex Interactions," *J. Am. Helicopter Soc.*, Vol. 34, No. 3, pp. 30-39, 1989.

Mantay, W. R., Campbell, R. L. and Shidler, P. A., "Full-Scale Testing of an Ogee Tip Rotor Helicopter Rotor," NASA CP-2052, May 1977.

Martin, R. M., Marcolini, M. A., Spelettstosser, W. R., and Schultz, K. J., "Wake Geometry Effects on Rotor Blade-Vortex Interaction Noise Directivity," NASA TP-3015, 1990.

Martin, R.M., "Acoustic Design Considerations: Review of Rotor Acoustic Sources," NASA N90-1258018, May 1989.

Martin, R.M., Splettstoesser, W.R., Elliott, J.W., and Schultz, K.J., "Advancing Side Directivity and Retreating Side Directivity Interactions of Model Rotor Blade-Vortex Interaction Noise," NASA Technical Paper 2784, 1988.

George Rotorcraft Noise
93-0592

McCroskey, W. J. and Goorjian, P. M., "Interactions of Airfoils with Gusts and Concentrated Vortices in Unsteady Transonic Flow," AIAA Paper No. 83-1691, 1983.

McVeigh, Michael A., Grauer, William K., and Paisley, David J., "Rotor/Airframe Interactions on Tiltrotor Aircraft", *J. Am. Helicopter Soc.*, pp. 43-51, July 1990.

Miller, P., and Wilson, M., "Wall Jets Created by Single and Twin High Pressure Jet Impingement," *Aeronautical Journal*, pp. 87-100, March 1993.

Myers, M. K. and Farassat, F., "Structure and Propagation of Supersonic Singularities from Helicoidal Sources," AIAA Paper No. 87-2676, 1987.

Norman, Thomas R., and Light, Jeffrey S., "Rotor Tip Vortex Geometry Measurements Using the Wide-Field Shadowgraph Technique", *J. Am.Helicopter Soc.*, pp. 40-50, April 1987.

Obermeier, F., "Numerical and Experimental Investigations on Aerodynamic Sound Generation due to Transonic Vortex-Rotor-Interaction," NATO-CCMS Symposium on Noise Aspects of Rotary Wing Aircraft, Monterey, 1991.

Paterson, R. W., Amiet, R. K. and Munch, C. L., "Isolated Airfoil - Tip Vortex Interaction Noise," *J. Aircraft*, Vol. 12, No. 1, pp. 34-40, 1975.

Paterson, R. W., Vogt, P. G., Fink, M. R., Munch, C. L., "Vortex Noise of Isolated Airfoils," *J. of Aircraft*, Vol. 10, 1973.

Pegg, R. J., Magliozzi, B. and Farassat, F., "Some Measured and Calculated Effects of Forward Velocity on Propeller Noise," ASME Paper 77-GT-70, 1977.

Plotkin, K. J. and Cantril, J. M., "Prediction of Sonic Boom at a Focus," AIAA Paper No. 76-2, 1976.

Rai, M. M., "Navier-Stokes Simulations of Blade-Vortex Interaction Using High-Order Accurate Upwind Schemes," AIAA Paper No. 87-0543, Jan. 1987.

Reid, D. C., "Rotarty Wind Noise," U.K. Military Presentation, NATO-CCMS Symposium on Noise Aspects of Rotary Wing Aircraft, Monterey, 1991.

Ringler, T.D., George, A.R. and Steele, J. B., "The Study of Blade-Vortex Interaction Sound Generation and Directionality," Proceedings of the AHS Technical Specialists' Meeting, October 1991.

Rutledge, Charles K., Coffen, Charles D., and George, Albert R., " A Comparative Analysis of XV-15 Tiltrotor Hover Test Data and WOPWOP Predictions Incorporating the Fountain Effect", Proceedings, AHS & Royal Aero. Soc. Intl. Technical Specialists Meeting on Rotorcraft Acoustics and Rotor Fluid Dynamics, Valley Forge, Pa., Oct. 15-17, 1991.

Sadler, S. G., "Development and Application of a Method for Predicting Rotor Free Wake Positions abd Resulting Rotor Blade Air Loads," NASA CR-1911, 1971.

Schmitz, F. H., "Rotor Noise," Aeroacoustics of Flight Vehicles: Theory and Practice, edited by H. Hubbard, NASA Reference Publication 1258, August 1991.

Schmitz, F. H. and Yu, Y. H., "Helicopter Impulsive Noise: Thereotical and Experimental Status," *J. Sound and Vibration*, Vol. 109, No. 3, pp. 361-422, 1986..

Schmitz, F. H. and Yu, Y. H., "Theoretical Modeling of High-Speed Helicopter Impulsive Noise," *J. Am. Helicopter Soc.*, Vol. 24, No. 1, pp. 10-19, 1979.

Scully, M. P., "Computation of Helicopter Rotor Wake Geometry and Its Influence on Rotor Harmonic Airloads," M.I.T. ASRL TR 178-1, March 1975.

Signor, D. B., Yamauchi, G. K., Mosher, M., Hagen, M. J., and George, A. R., "Effects of Ingested Atmospheric Turbulence on Measured Tail Rotor Acoustics", Presented at the 48th Annual Forum of the AHS, Washington D.C., June 3-5, 1992.

Sim, B. W.-C. and George, A. R., "A Study of Propfan Noise Propagation," AIAA Paper No. 93-0602, Jan. 1993.

Simonich, J.C., Amiet, R.K., Schlinker, R.H., and Greitzer, E.M., "Rotor Noise Due to Atmospheric Turbulence Ingestion-Part I: Fluid Mechanics", *J. Aircraft*, Vol. 27, No. 1, pp. 7-14, January 1990.

Sirinivasan, G. R. and McCrosky, W. J., "Numerical Simulations of Unsteady Airfoil-Vortex Interactions," *Vertica*, Vol. 11, No. 1/2, pp. 3-28, 1987.

Sirinivasan, G. R., McCrosky, W. J., Baeder, J. D., "Aerodynamics of Two-Dimensional Blade-Vortex Interaction," AIAA Paper No. 85-1560, 1985.

Splettstosser, W. R., Lehmann, G. and van der Wall, B., "Higher Harmonic Control of a Model Helicopter Rotor to Reduce Blade-Vortex interaction Noise," *Z Flugwiss Weltraumforch*, Vol. 14, pp. 109-116, 1990.

Splettstoesser, W. R., Schultz, K. J. and Martin, R. M., "Rotor Blade-Vortex Interaction Impulsive Noise Source Localization," *AIAA Journal*, Vol. 28, No. 4, pp. 593-600, April 1990.

Splettstoesser, W. R., Schultz, K. J., Schmitz, F. H. and Boxwell, D. A., "Model Rotor High-Speed Impulsive Noise - Parametric Variations and Full-Scale Comparisons," Presented at 39th Annual Forum of the AHS, St. Louis, May 9-11, 1983.

Tadghighi, H., Holz, R., Farassat, F. and Lee, Y.-J., "Development of a Shock Noise Prediction Code for High-Speed Helicopters - The Subsonically Moving Shock," Presented at the 47th Annual Forum of the AHS, Phenoix, Arizona, May 1991.

Tadghighi, H., "An Analytical Model for Prediction of Main Rotor/Tail Rotor Interaction Noise," AIAA Paper No. 89-1130, 1989.

Tam, C. K. W. and Yu, J. C., "Trailing Edge Noise," AIAA Paper No. 75-489, 1975.

Tangler, J. L., "Schlieren and Noise Studies of Rotors in Forward Flight," Presented at the 33rd Annual Forum of the AHS, Washingtion D.C., May 1977.

Tijdeman, H., "Investigations of Transonic Flow Around Oscillating Airfoils," NLR Rep 77090-U, 1977.

Wanner, J-C.L., Valee, J., Vivier, C. and Thery., "Theoretical and Experimental Studies of the Focus of Sonic Booms," *J. Acoust. Soc. Am.*, Vol. 52, 1972.

Weir, D. S. and Golub, R. A., "Status of the ROTONET Prediction System," Presented at the 6th Annual NASA/AHS Review, Washington, D.C., October 6-8, 1989.

White, R. P., Jr., "The Status of Rotor Noise Technology," *J. Am. Helicopter Soc.*, Vol. 25, No. 1, pp. 22-29, Jan. 1980.

Widnall, S. E., "Helicopter Noise due to Blade-Vortex Interaction," *J. Acoust. Soc.Am.*, Vol. 50, No. 1, part 2, pp. 354-365, 1971.

Wright, S. E., "Sound Radiation from a Lifting Rotor Generated by Asymmetric Disc Loading," *J. Sound and Vibration*, Vol. 9, pp. 223-240, 1969.

To Appear in: ASME Journal of fluids Engineering, December 1993 issue

Tilt Rotor Broadband Hover Aeroacoustics

C. D. Coffen*
United Technologies Research Center
East Hartford, CT 06108

A. R. George†
Cornell University
Ithaca, NY 14853

Abstract

To improve the acoustic characteristics of tilt rotor aircraft, the dominant noise mechanisms must be understood. Towards this goal, a method was developed to identify and predict the dominant broadband noise mechanism of a hovering tilt rotor. Predictions are presented for a range of azimuthal observer locations and polar observer angles and are compared to NASA full scale tilt rotor hover noise data. Comparisons between experiment and prediction indicate that the polar and azimuthal directionality trends are captured. The predicted sound spectrum levels are generally within 5 dB of the experiment. The results of this study indicate that the highly turbulent recirculating fountain flow is the dominant broadband noise mechanism for a tilt rotor aircraft in hover.

1 Introduction

This paper will report on some important progress in understanding and predicting the dominant source of broadband noise generated by a hovering tilt rotor aircraft. This mechanism has been identified as unsteady lift on the rotor blades generated by the reingestion of the highly turbulent recirculating fountain flow.[1] Experiments were conducted on a twelfth scale model tilt rotor in hover mode in order to characterize the unsteadiness, turbulence intensity, integral scale, and spatial extent of the fountain flow. The results of our experimental study (Coffen et al., 1991) are used as input to a modified version of Amiet's noise prediction code (Amiet, 1989). Several analytical techniques are available for predicting the broadband noise due to rotor interaction with a turbulent inflow field: Homicz and George (1974), George and Kim (1977), and Amiet (1976). Amiet's method is used as a starting point because it is the only analysis which can be modified to account for azimuthally varying inflow turbulence. This analysis also accounts for blade-to-blade correlations, includes rapid distortion theory (not used in the current study), and has been shown to accurately predict turbulence ingestion noise in previous studies (Amiet, 1976; Simonich et al., 1989). Of special interest to the celebration of Professor W. R. Sears' 80th birthday is Amiet's use of the classical Sears function (Sears, 1939) as the airfoil response function to turbulent inflow.

The fundamental geometry of the tilt rotor aircraft, shown in figure 1, consists of prop-rotors mounted on tiltable nacelles which are located at or near the tips of a fixed (non-tilting) wing. The prop-rotor is sufficiently large so that the benefits of low disk loading are gained for efficient hover flight. The prop-rotor is designed to provide the desired performance balance between the axial-flow hover requirement and the axial-flow airplane mode requirement (Rosenstein and Clark, 1983; McVeigh et al., 1983; Paisley, 1987). Tilt rotor aircraft are being seriously considered as future commercial transports. Their unique design allows them to take-off and land vertically (or with very short ground rolls) then convert into

*Assistant Research Engineer

†Professor of Mechanical & Aerospace Engineering

[1] Discrete noise prediction techniques, hover flow characterization and visualization, and blade vortex interaction noise are discussed in Coffen and George (1990), Coffen et al. (1991), Rutledge et al. (1991), Coffen (1992), and George et al. (1992).

conventional airplane mode for cruise. The need for only small verti-ports in strategic locations, such as near city centers, make the tilt rotor's use very attractive. The limiting factors for tilt rotor aircraft commercialization include cost, safety, the existence of verti-ports, and noise. Clearly, with the possibility of operating close to densely populated areas, it is imperative that the tilt rotor's noise radiation be acceptable to the public.

The importance of tilt rotor acoustics makes it vital to better understand the noise mechanisms. In addition to exhibiting most of the noise mechanisms of a conventional helicopter, the tilt rotor is also affected by other noise mechanisms. The tilt rotor introduces a number of unique prop-rotor/airframe aerodynamic interactions that result in important noise and performance problems. Fortunately, tilt rotors can be operated with more degrees of freedom than helicopters and thus may have more potential for operational noise reductions (George et al., 1989). Minimizing the acoustic signal can be accomplished in two ways: by reduction in the strength of the basic mechanisms, and by understanding and then controlling the strong directionality of the observed radiation. Improved understanding of tilt rotor noise will aid in minimizing noise radiation for the existing tilt rotor and help determine the proper design changes for future generations of tilt rotor aircraft.

2 Tilt Rotor Fountain Effect

The operational configuration of a hovering tilt rotor aircraft is such that the presence of the wing and fuselage beneath the rotor strongly affects the aerodynamics by introducing complex unsteady recirculating flows. Figure 1 shows a simplified schematic of this fountain flow while figure 2 is an actual photo from a flow visualization study conducted on a one-twelfth scale model tilt rotor (Coffen et al., 1991). The wing and fuselage provide a partial ground plane in the near wake which causes the development of an inboard-bound spanwise flow over the wing and fuselage surface. At the aircraft's longitudinal plane of symmetry, the opposing flows collide, producing an unsteady "fountain flow" with upward velocity components. This fountain flow, characterized by higher than ambient turbulence intensity levels and smaller integral scale, is then reingested by the rotors, resulting in azimuthally varying inflow turbulence levels. The interaction of the rotors with this highly turbulent spatially non-uniform flow causes significant broadband noise which is radiated preferentially to the rear of the aircraft (the direction of motion as the blade passes through the fountain).

3 Summary of Amiet's Method

Amiet's method for predicting noise generated by turbulent flow into a rotor has been documented previously in the literature (Amiet, 1975; Amiet, 1976; Amiet, 1989). The following is a summary of the theory involved in the method and includes a brief description of the implementation of the classical Sears function. Initially, Amiet's analysis was applied to the case of an airfoil convecting rectilinearly through a turbulent flow field (Amiet, 1975). Amiet later extended this analysis to include the effects of the rotary motion of an airfoil (propeller or rotor blade) (Amiet, 1976). In this study, Amiet's method was further modified in order to account for azimuthally varying inflow turbulence.

3.1 Airfoil in Rectilinear Motion

An airfoil passing through a turbulent flow field experiences an unsteady loading due to the fluctuating airfoil angle of attack. This unsteady loading translates into unsteady surface pressures which propagate to the far field as noise. Amiet's analysis assumes that a vertical gust convects perpendicular to the leading edge of a flat plate airfoil. Linearized theory is assumed throughout the analysis. When the gust impinges on the airfoil, a surface dipole distribution is induced to oppose the gust flow and satisfy the condition of no flow through the airfoil surface. This surface dipole distribution creates a pressure jump across the upper and lower surfaces which acts as an effective distributed force on the airfoil. The

far-field noise can be calculated by noting that a force imposed by the fluid produces a dipole pressure field response (acoustic sources). These acoustic dipole sources are equal in strength to the force induced on the airfoil by the convecting turbulent gusts. Amiet's analysis provides an expression for the far-field acoustic power spectral density in terms of the turbulence velocity spectrum and the airfoil response function. The product of these two functions can be described as the transfer function between the turbulent inflow velocity fluctuations and the far-field acoustics:

$$S_{pp}(\underline{x},\omega) = \left(\frac{\omega z \rho_0 b}{c_0 \sigma^2}\right)^2 \pi U d \left|\mathcal{L}\left(x, k_x, \frac{\omega y}{c_0 \sigma}\right)\right|^2 \Phi_{ww}\left(k_x, \frac{\omega y}{c_0 \sigma}, M\right) \tag{1}$$

3.2 Airfoil Response Functions: The Sears Function

The rotor blades' unsteady lift response to an incident gust is the fundamental source of the turbulence ingestion noise mechanism. At low Mach number and reduced frequency, the Sears function can be used with good accuracy (an alternate response function is used for larger values of Mach number and reduced frequency). Amiet shows that the effective lift, $\mathcal{L}$, can be expressed as:

$$\mathcal{L}\left(x, k_x, \frac{\omega y}{c_0 \sigma}\right) = \frac{1}{\beta} S\left(\frac{k_x}{\beta^2 b}\right) e^{i\frac{k_x}{\beta^2 b} f(M)} \left(J_0\left(\frac{M k_x x}{b\beta^2 \sigma}\right) - i J_1\left(\frac{M k_x x}{b\beta^2 \sigma}\right)\right) \tag{2}$$

In this expression, S is the classical Sears function described in the following: Sears and Keuthe (1939), Von Kármán and Sears (1938), and Sears (1940). This application demonstrates the practical importance of Sears' work on unsteady flow problems. A numerical calculation of this analysis would not be possible without the groundwork provide by Sears and others in understanding the fundamentals of airfoil response to unsteady flows. One should also note that while there are several different techniques for calculating turbulence ingestion noise, the methods of Homicz and George (1974), and George and Kim (1977) also make use of the Sears function in their respective analyses.

3.3 Airfoil in Rotary Motion

A fundamental difference between Amiet's method and the other noted methods is that the rotary motion of the blade element is approximated as a series of rectilinear motions. Two effects cause the observer fixed instantaneous sound spectrum of a rotating source to vary periodically in time. First, the orientation of the source radiation directivity relative to a fixed observer changes as the blade rotates. This causes the spectrum amplitude to modulate at the rotor rotational frequency. Second, the retarded time effects, due to the source alternately moving away and towards the observer, cause an alternate compression and dilation of the time scale of the signal. Finding the exact spectrum of a broadband noise signal modified in these two ways would be difficult. An approximation can be made by assuming that the frequencies of interest are much greater than the rotor rotational frequencies. The rotor rotation period, T, is divided into short time segments, ΔT. A spectrum is calculated for each time segment during which it is assumed that the rotor blade is moving rectilinearly. These "instantaneous" spectra are averaged resulting in a spectrum which is the equivalent of the output of a constant bandwidth spectrum analyzer that has insufficient resolution to display the rotation harmonics. The technique for calculating the azimuthally averaged spectrum of a rotating source modeled by rectilinear motion is described in Amiet (1976) and Schlinker and Amiet (1981) with the result expressed as:

$$S_{pp}(\underline{x},\omega_0) = \frac{1}{2\pi}\int_0^{2\pi} \frac{\omega}{\omega_0} S_{pp}(\underline{x},\omega_0,\gamma) d\gamma \tag{3}$$

Equation (3) is used with equation (1) to predict the far-field acoustics of turbulence ingestion noise.

4 Calculation Procedure (Modified Amiet's Method)

Amiet's method can be used to calculate the noise due to azimuthally varying turbulence because the analysis makes the rectilinear motion approximation. In the numerical implementation, the blade span is discretized into segments and the blade rotation is reduced to a series of rectilinear motions which approximate the rotary trajectory of the blade. Spatial variations were implemented by associating appropriate turbulence characteristics with each blade segment and azimuthal location. The implementation requires keeping track of where the observer is located with respect to the motion of the blade and the blade's azimuthal location, because the Doppler amplification factor changes as the blade rotates towards and away from the observer. This relationship determines the azimuthal directionality of the broadband noise as the observer's location relative to the blade as it passes through the high levels of turbulence in the fountain flow determines the relative amplitude of the broadband noise.

The azimuthally varying turbulence was defined in such a way as to approximate the measured spatial variations in turbulence properties measured in the one-twelfth scale model experiments. Figure 3 indicates the spatial variations in turbulence level in the inflow field. The contour levels are the measured quantity $\sqrt{(u'^2 + v'^2 + w'^2)/3}$ and are only useful to identify the spatial extent of the highly turbulent recirculating flow. The vertical gust component of the turbulence, w', which causes the unsteady blade loading, was not directly deduced from this data as the measurements also include the fluctuating velocity due to the potential flow generated by the blade passing underneath the hot wire probe. However, the yellow and green shading clearly indicates a region of highly turbulent inflow which the rotor blade encounters as it rotates towards the rear of the aircraft.

4.1 Turbulence Spectra

Amiet's method assumes that the turbulence velocity spectrum, $\Phi_{ww}(k_x, k_y, k_z)$, is related to $E(k)$, the Von Kármán energy spectrum as function of the magnitude of the wave vector, k, by

$$\Phi_{ww}(k_x, k_y, k_z) = \frac{E(k)}{4\pi k^2}\left(1 - \frac{k_z^2}{k^2}\right) \tag{4}$$

The accuracy of the Von Kármán energy spectrum vis-a-vis the actual inflow turbulence is an important assumption in predicting the acoustic spectra. This assumption was examined by comparing an experimentally obtained fountain turbulence spectrum to the Von Kármán spectrum as follows: The longitudinal spectrum of the turbulence, $F_{11}(k)$, for the one-twelfth scale model was obtained from the power spectral density of the inflow which was measured with a hot wire placed in the highly turbulent region over the wing. Assuming isotropic turbulence, the energy spectrum is related to the the longitudinal spectrum by:

$$E(k) = k^3 \frac{d}{dk}\left(\frac{1}{k}\frac{d}{dk}F_{11}(k)\right) \tag{5}$$

Integrating twice with respect to k and setting the constants of integration to zero gives an analytical expression for the longitudinal spectrum based on the Von Kármán energy spectrum. Figure 4 is a comparison between the experimental data and the Von Kármán spectrum and exhibits good agreement for wave numbers less than $10^3 m^{-1}$. One should note that the discrete peaks in the experimental spectra are related to the blade passing frequencies and are caused by the potential field of the rotating blade. In calculating $F_{11}(k)$ for the Von Kármán spectrum, the *rms* turbulence velocity is obtained by integrating the area under the experimentally obtained $F_{11}(k)$ of inflow velocity and the turbulent length scale is assumed to be equal to the chord of the rotor blade. For the purposes of the XV-15 acoustic predictions presented below, w' in the reingestion area of the rotor disk is assumed to scale from the one-twelfth scale experiment with the rotor disk area averaged convection velocity, W. This velocity is calculated from the known thrust of the XV-15 in hover, and is calculated from inflow measurements in the experiment. The turbulence length scale is assumed to scale with blade chord length. For regions of the rotor disk

not in the reingestion zone, representative atmospheric turbulence is assumed: the integral scale is taken to be 90% of the hover height and the *rms* turbulence velocity is given the typical value of 1 m/s.

5 Predicted Spectra

Predicted and measured noise spectra are presented in figures 6 - 9 for four polar observer angles. Each of these figures has curves for experiment[2] and prediction for three azimuthal observer locations: front, side, and rear aircraft acoustics (see figure 5 for directionality definitions). These predictions are in good agreement with the experimental data as both the polar and azimuthal directionality trends are captured. The predicted spectrum levels are generally within 5 dB of experiment with the following exceptions: The **front** acoustic predictions are 5 - 15 dB low over a portion of the spectrum for the 7.2°, 12.7°, and 23° polar angle observer locations. The part of the spectrum where the predictions do not agree increases for lower aircraft hover heights (smaller polar angles). At these lower hover heights, there may be some recirculation due to the ground plane which would increase the ambient turbulence intensities above the 1 m/s assumed for the predictions, and result in higher than predicted noise levels. One should note that the low frequency discrete noise is due to the mean flow of the fountain and is not treated in this paper. Analysis and predictions of discrete noise due to the fountain mean flow are presented in Coffen and George (1990), Rutledge et al. (1991), and Coffen (1992).

The good agreement between the predictions and experimental data indicate that the highly turbulent recirculating fountain flow has been correctly identified as the dominant broadband noise mechanism for a hovering tilt rotor. The predictions capture the azimuthal directionality trends; the levels are higher for an observer behind the aircraft with the levels decreasing as the observer location is moved around the aircraft to the front. The effect of azimuthally varying turbulence characteristics on the noise directionality is further illustrated in figure 9 which has a prediction based on uniform atmospheric turbulence (labeled **Uniform Turbulence**). This prediction underpredicts the noise levels by 10 - 25 dB depending on frequency and is independent of azimuthal observer location. The azimuthal variations in noise levels can be explained by aeroacoustic theory which shows that the noise is amplified in the direction that the source is moving (Lowson, 1965). Because the blade is moving towards the rear of the aircraft as it passes through this highly turbulent region, noise is radiated preferentially to the rear with levels decreasing to a minimum at the front of the aircraft where the blades are moving away from the observer as they pass through the reingestion zone.

6 Conclusion

Modifications to Amiet's method of predicting turbulence ingestion noise have resulted in a means of predicting broadband rotor noise generated by azimuthally varying inflow turbulence. For the results presented here, the azimuthal variations are based on one-twelfth scale model tilt rotor hover experiments. Noise predictions based on this method compare well, both levels and trends, with full scale hover acoustics tests conducted by NASA on the XV-15. The good correlation between these broadband predictions and experiment indicates that the highly turbulent, reingested inflow is the dominant broadband noise mechanism for a hovering tilt rotor. As alluded to previously, these strong directional dependences can be taken advantage of to minimize the aircraft's operational noise annoyance. The pilot should operate the aircraft such that the rear of the aircraft faces away from areas that would be most adversely affected by the noise.

Acknowledgements

This research was supported by NASA Ames Grant NAG-2-554 and partly by the NASA-Cornell University Space Grant Program. We also acknowledge many helpful conversations with Roy K. Amiet

[2] Rutledge et al. (1991) contains a complete description of the experimental method used to obtain the full scale acoustic measurements.

and the crucial contributions of Charles K. Rutledge (NASA Langley).

Bibliography

Amiet, R. K., 1975, "Acoustic Radiation from a Airfoil in a Turbulent Stream," *Journal of Sound and Vibration*, Vol. 41, pp. 407-420.

Amiet, R. K., 1976, "Noise Produced by Turbulent Flow into a Propeller or Helicopter Rotor," AIAA Paper 76-560.

Amiet, R. K., 1989, "Noise Produced by Turbulent Flow into a Rotor: Theory Manual for Noise Calculation," NASA CR 181788.

Coffen, C. D., and George, A. R., 1990, "Analysis and Prediction of Tilt Rotor Hover Noise," *Proceedings of the 46th Annual Forum & Technology Display for the American Helicopter Society,* Washington, D.C.

Coffen, C. D., and George, A. R., Hardinge, H., and Stevenson, R., 1991, "Flow Visualization and Flow Field Measurements of a 1/12 Scale Tilt Rotor Aircraft in Hover," *Proceedings of the American Helicopter Society Technical Specialist' Meeting,* Philadelphia, PA.

Coffen, C. D., 1992, "Tilt Rotor Hover Aeroacoustics." Masters Thesis, Department of Mechanical and Aerospace Engineering, Cornell University, Ithaca, NY; also NASA CR 177598.

Homicz, G. F., and George, A. R., 1974, "Broadband and Discrete Frequency Radiation from Subsonic Rotors," *Journal of Sound and Vibration*, Vol. 36, pp. 151-177.

George, A. R., Kim, Y. N., 1977, "High Frequency Broadband Rotor Noise," AIAA Journal 15, No. 11, pp. 538-545. Also AIAA Paper No. 76-561 (1976).

George, A. R., 1984, "Comparisons of Broadband Noise Mechanisms, Analyses, and Experiments on Rotors," Journal of Aircraft, 21, No. 8, pp 583-592.

George, A. R., Smith, C., Maisel, M., and Brieger, J., 1989, "Tilt Rotor Aircraft Aeroacoustics," *Proceedings of the 45th Annual Forum & Technology Display of the American Helicopter Society,* Boston, MA.

George, A. R., Coffen, C. D., and Ringler, T. D., 1992, "Advances in Tilt Rotor Noise Prediction," DGLR/AIAA Paper 92-02-087. *Proceedings of the DGLR/AIAA 14th Aeroacoustics Meeting,* Achen, Germany.

Lowson, M. V., 1965, "The Sound Field of Singularities in Motion," *Proceedings of the Royal Society of London*, Series A, Vol. 286, pp. 559-572.

McVeigh, M. A., Rosenstein, H., and McHugh, F. J., 1983, "Aerodynamic Design of the XV-15 Advanced Composite Tilt Rotor Blade," *Proceedings of the 39th Annual Forum of the American Helicopter Society.*

McVeigh, M. A., Grauer, W. K., and Paisley, D. J., 1988, "Rotor/Aircraft Interactions on Tiltrotor Aircraft," *Proceedings of the 44th Annual Forum of the American Helicopter Society.*

Paisley, D. J., 1987, "Rotor Aerodynamics Optimization for High Speed Tilt Rotors," *Proceedings of the 43rd Annual Forum of the American Helicopter Society.*

Rosenstein, H., and Clark, R. 1983, "Aerodynamic Development of the V-22 Tilt Rotor," AIAA Paper No. AIAA-86-2678.

Rutledge, C. K., Coffen, C. D., and George, A. R., 1991, "A Comparative Analysis of XV-15 Tilt Rotor Hover Test Data and WOPWOP Predictions Incorporating the Fountain Effect," *Proceedings of the American Helicopter Society Technical Specialist' Meeting,* Philadelphia, PA.

Schlinker, R. H., and Amiet, R. K., 1981, "Helicopter Rotor Trailing Edge Noise," NASA CR 3470.

Sears, W. R., and Keuthe, A. M., 1939, "The Growth of the Circulation of an Airfoil Flying Through a Gust," *Journal of Aeronautical Sciences,* Vol. 6, pp. 376-378.

Sears, W. R., 1940, "Some Aspects of Non-Stationary Airfoil Theory and its Practical Application," *Journal of Aeronautical Sciences,* Vol. 8, pp. 104-108.

Simonich, J. C., Schlinker, R. H., and Amiet, R. K., 1989, "Experimental Assessment of Helicopter Rotor Turbulence Ingestion Noise in Hover," NASA CR 181792.

Von Kármán, T., and Sears, W. R., 1938, "Airfoil Theory for Non Uniform Motion," *Journal of Aeronautical Sciences,* Vol. 5, pp. 379-390.

Appendix: List of Symbols

b	semi-chord
d	semi-span
c_0	sound speed
ρ_0	ambient fluid density
U	free stream velocity
W	mean convection velocity through the rotor
u', v', w'	Cartesian components of rms velocity
J_0, J_1	Bessel functions of the first kind
k	magnitude of wave number vector
k_x, k_y, k_z	Cartesian wave numbers of turbulence
$\mathcal{L}$	effective lift
M	free stream Mach number
$\underline{M_t}$	Mach number of the source relative to the observer
$\underline{M_r}$	Mach number of the source relative to the ambient fluid
S_{pp}	PSD of far field sound
S	Sears function
$\underline{x}$	observer location with respect to the rotor hub
x, y, z	chordwise, spanwise, and normal Cartesian coordinates
β	$\sqrt{1-M^2}$
σ	$\sqrt{x^2+\beta^2(y^2+z^2)}$
ω	circular frequency
ω_0	Doppler shifted frequency
γ	azimuthal angle
Φ_{ww}	velocity spectrum of turbulence
E	Von Kármán energy spectrum of turbulence
F_{11}	longitudinal velocity spectrum of turbulence
$f(M)$	$(1-\beta)lnM + \beta ln(1+\beta) - ln2$
$\underline{QS}$	unit vector from the observer to the retarded source

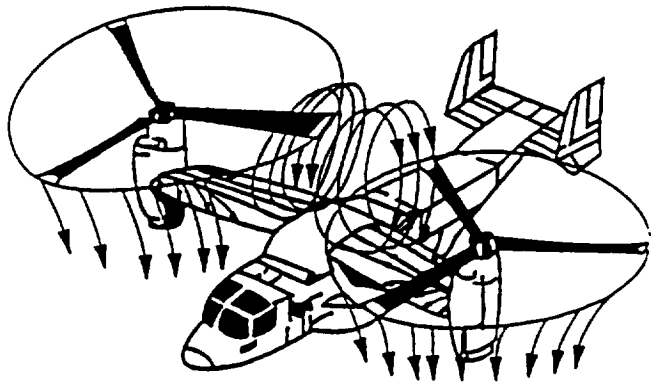

Figure 1: Schematic of the hover mode wake/flow patterns (McVeigh et al., 1988).

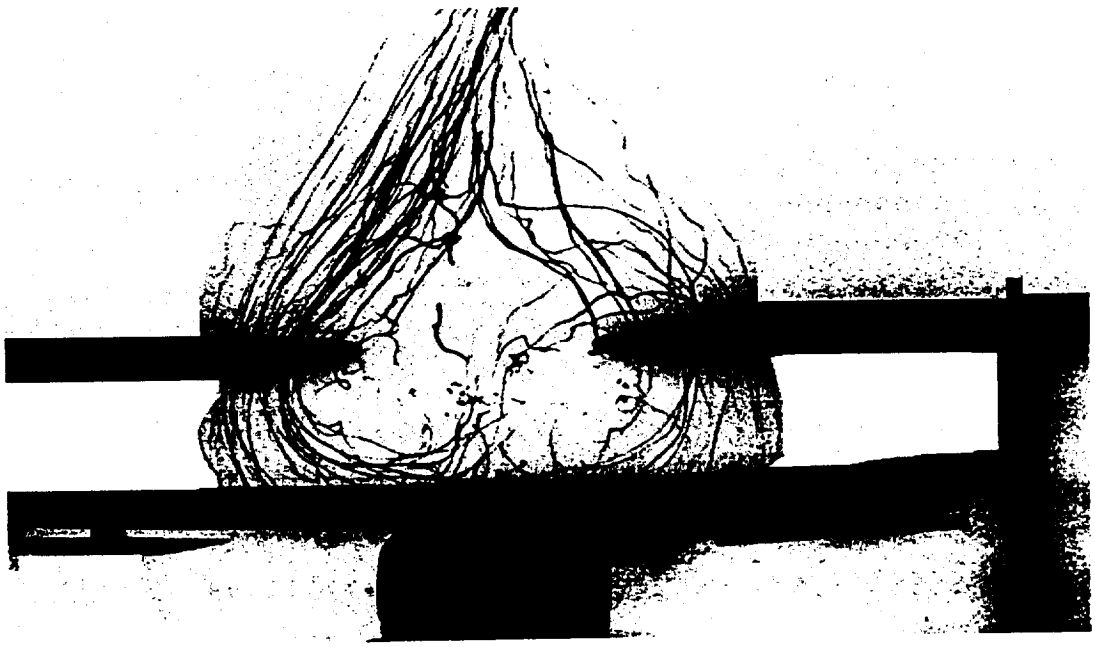

Figure 2: Computer enhanced digitized photo of the fountain flow. Viewer is in front of the model looking down the fuselage. Helium filled soap bubbles are injected over the center of the wing on the rotor/rotor axis. This illustrates the spanwise flow, fountain height and recirculation. 1/2 second exposure time.

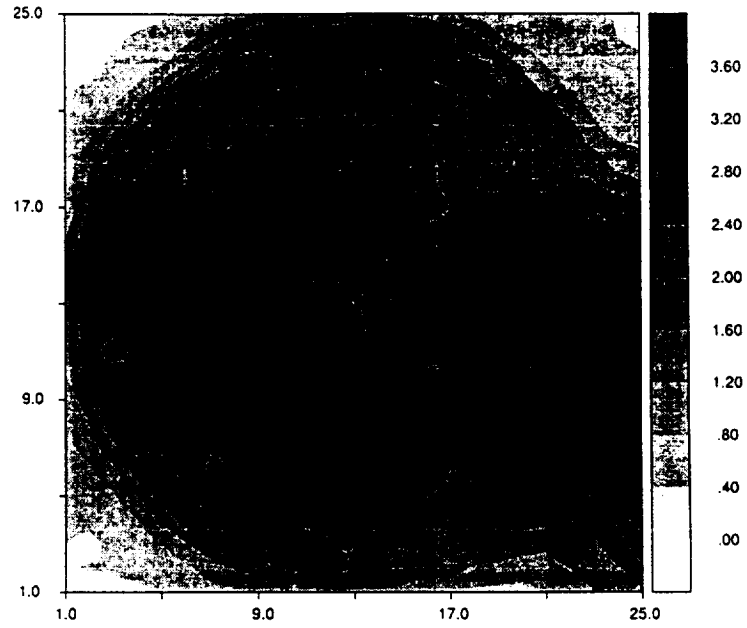

Figure 3: Contour plot of *rms* inflow velocity: $\left(\frac{u'^2+v'^2+w'^2}{3}\right)^{0.5}$ (m/s). Port rotor, rotates clockwise, 24 inch diameter blade. Yellow and green shading corresponds to high levels of turbulence in the reingestion zone over the wing (the fuselage is to the right of the plot with the tail towards the bottom of the page).

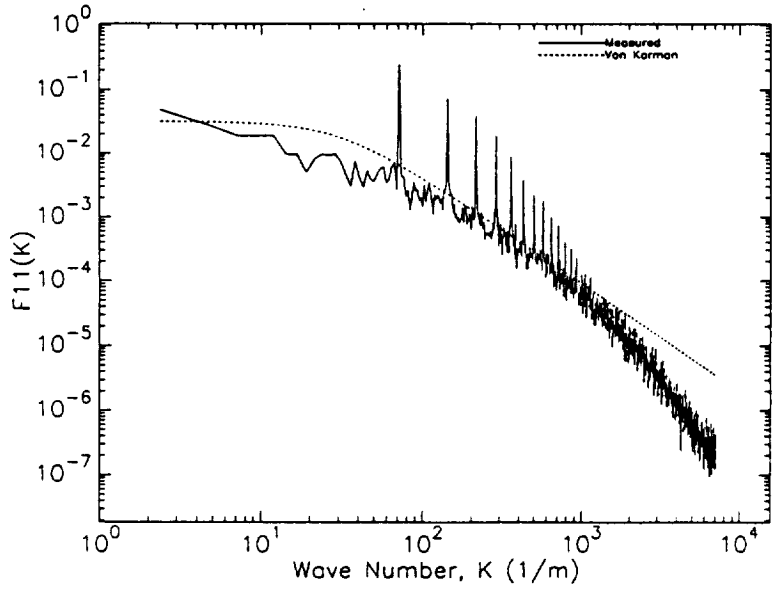

Figure 4: Comparison of Measured and Von Kármán longitudinal velocity spectrum of fountain flow turbulence for the 1/12 scale model tilt rotor.

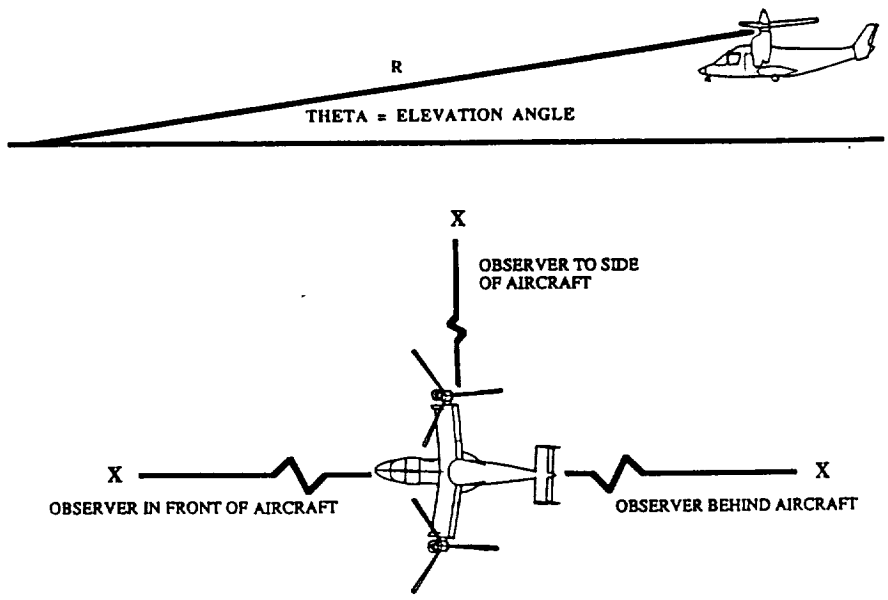

Figure 5: Schematic of observer locations for the predictions and experiment.

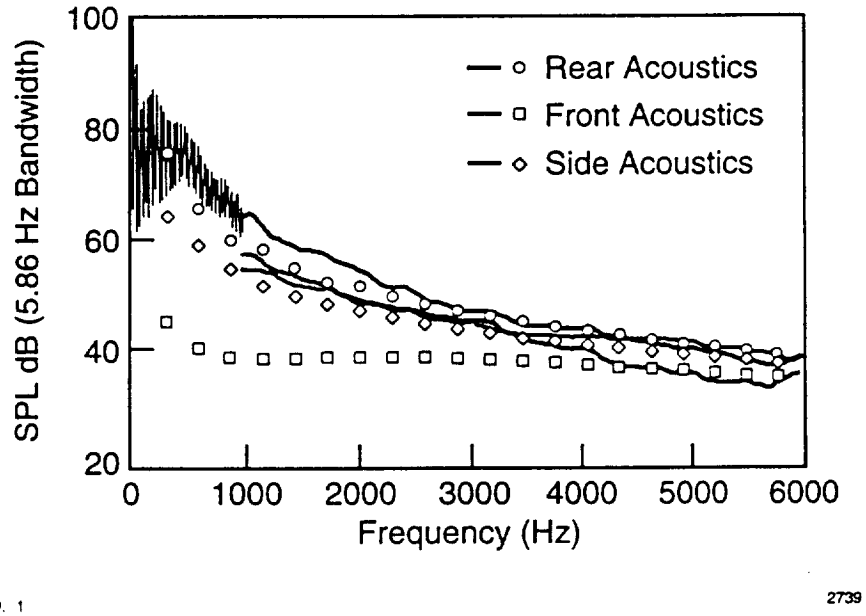

Figure 6: Comparison of experimental and predicted broadband noise spectra. Rear, side, and front aircraft acoustics, $\theta = 7.2°$ (50' hover height). Lines are experiment, symbols are prediction. The broadband part of the experimental spectra are faired, and front and side spectra are truncated below 1000 Hz.

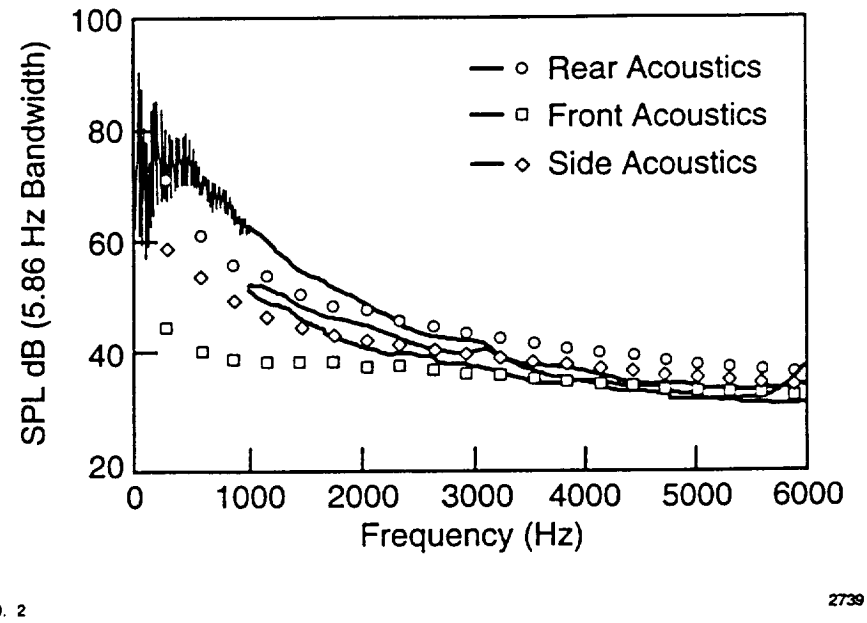

Figure 7: Comparison of experimental and predicted broadband noise spectra. Rear, side, and front aircraft acoustics, $\theta = 12.7°$ (100' hover height). Lines are experiment, symbols are prediction. The broadband part of the experimental spectra are faired, and front and side spectra are truncated below 1000 Hz.

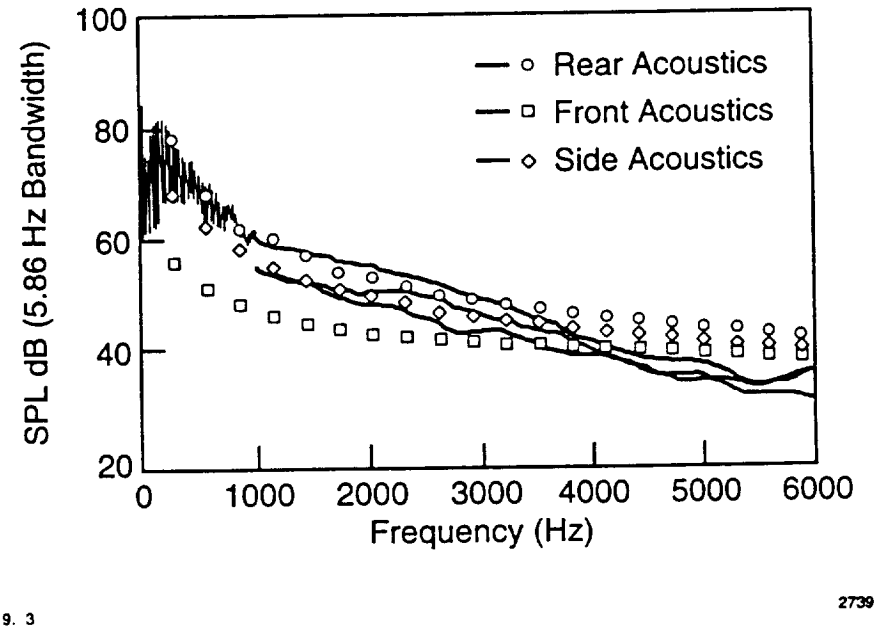

Figure 8: Comparison of experimental and predicted broadband noise spectra. Rear, side, and front aircraft acoustics, $\theta = 23.0°$ (200' hover height). Lines are experiment, symbols are prediction. The broadband part of the experimental spectra are faired, and front and side spectra are truncated below 1000 Hz.

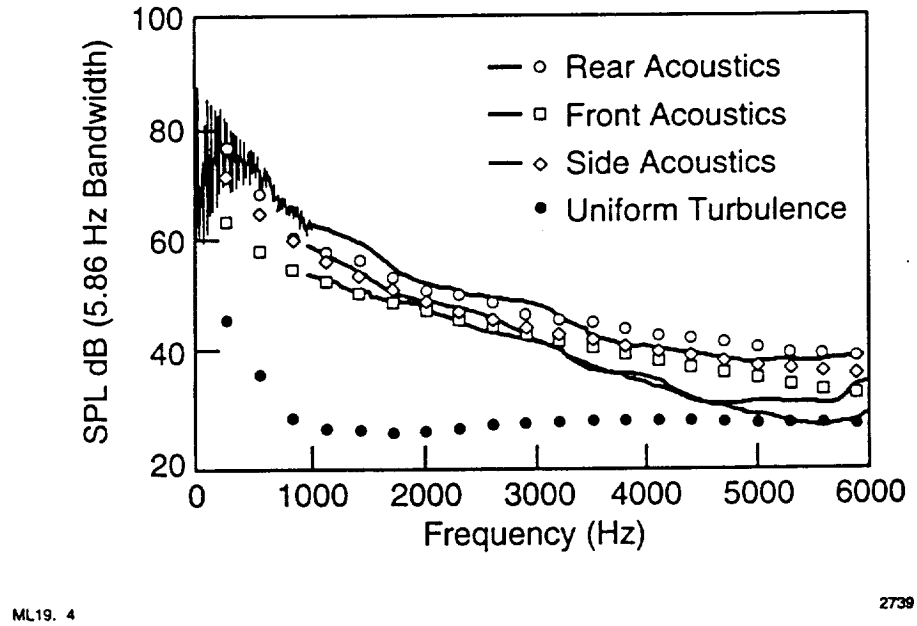

Figure 9: Comparison of experimental and predicted broadband noise spectra. Rear, side, and front aircraft acoustics, $\theta = 45.7°$ (500' hover height). Lines are experiment, symbols are prediction. The broadband part of the experimental spectra are faired, and front and side spectra are truncated below 1000 Hz.